A THESIS SUBMITTED TO
THE GRADUATE SCHOOL OF NATURAL AND APPLIED SCIENCES
OF ÇANKIRI KARATEKİN UNIVERSITY

INHIBITORY ACTIVITY OF SILVER NANOPARTICLES ON *STAPHYLOCOCCUS AUREUS* GROWTH AND α-HEMOLYSIN GENE EXPRESSION

IN PARTIAL FULFILLMENT OF THE REQUIREMENTS
FOR
THE DEGREE OF MASTER OF SCIENCE
IN
BIOLOGY

BY

AI-HASAN ALI YOUSIF AL-ABAYECHI

ÇANKIRI

2023

INHIBITORY ACTIVITY OF SILVER NANOPARTICLES ON *STAPHYLOCOCCUS AUREUS* GROWTH AND α-HEMOLYSIN GENE EXPRESSION

By AI-Hasan Ali Yousif AL-ABAYECHI

December 2023

We certify that we have read this thesis and that in our opinion it is fully adequate, in scope and in quality, as a thesis for the degree of Master of Science

Advisor : Asst. Prof. Dr. Zehra CAN KARAHAN
Co-Advisor :Asst. Prof. Dr.Meethaq Sattar ABOOD

Examining Committee Members:

Chairman : Asst. Prof. Dr. Zehra CAN KARAHAN
Biology
Çankırı Karatekin University

Member : Asst. Prof. Dr. Esin KINAY
Biology
Ahi Evran University

Member : Asst. Prof. Dr. Filiz SARIKAYA PEKACAR
Biology
Çankırı Karatekin University

Approved for the Graduate School of Natural and Applied Sciences

Prof. Dr. Hamit ALYAR
Director of Graduate School

I hereby declare that all information in this document has been obtained and presented in accordance with academic rules and ethical conduct. I also declare that, as required by these rules and conduct, I have fully cited and referenced all material and results that are not original to this work.

AI-Hasan Ali Yousif AL-ABAYECHI

ABSTRACT

INHIBITORY ACTIVITY OF SILVER NANOPARTICLES ON *STAPHYLOCOCCUS AUREUS*GROWTH AND α-HEMOLYSIN GENE EXPRESSION

AI-Hasan Ali Yousif AL-ABAYECHI

Master of Science in Biology

Advisor: Asst. Prof. Dr. Zehra CAN KARAHAN

Co-Advisor: Asst. Prof. Dr. Meethaq Sattar ABOOD

December 2023

This study aimed to isolate *S. aureus* from clinical samples, synthesize silver nanoparticles, and evaluate their antibacterial activity against *S. aureus*, as well as their ability to inhibit the expression of the α-hemolysin virulence gene. A total of 250 clinical samples were collected, including urine, burns, and sputum samples. Culturing, biochemical tests, the API20 assay, the Vitek2 system, and PCR were used to identify *S. aureus* isolates. Silver nanoparticles (AgNPs) were synthesized by the chemical reduction method and characterized by UV-vis spectroscopy, scanning electron microscopy (SEM), X-ray diffraction analysis (XRD), and Fourier transform infrared spectroscopy (FT-IR). Antibacterial activity was measured by minimum inhibitory concentration (MIC), minimum bactericidal concentration (MBC), and agar-well diffusion assay. Real-time PCR was used to evaluate the effect of AgNPs on α-hemolysin gene expression. Out of 250 samples, 44 (17.6%) were positive for *S. aureus*. There was no significant difference in isolation rates between sample types, genders, or age groups. AgNPs showed good antibacterial activity with inhibition zones up to 14.41 mm and MIC and minimum bactericidal concentration values of 8 and 64 μg/mL, respectively. Exposure to AgNPs significantly downregulated *S. aureus* α-hemolysin gene expression compared to untreated controls. To find out how AgNPs affected the production of virulence factors, real-time PCR was used to measure the levels of expression of the HLA gene that codes for α-hemolysin before and after being exposed to nanoparticles. The results showed that AgNPs significantly decreased HLA expression in *S. aureus* isolates compared to controls

that were not treated. This indicates the ability of AgNPs to suppress virulence in addition to their antibacterial effects. Finally, chemically synthesized AgNPs showed strong antibacterial and antivirulence properties against clinical *S. aureus* isolates, which shows how useful they could be as a medicine. The results warrant further studies into the exact mechanisms of AgNP antibacterial and antivirulence action. Overall, this study demonstrates the promise of AgNPs as a treatment approach for *S. aureus* infections.

2023, 90 pages

Keywords: Silver nanoparticles, α-Hemolysin gene, *Staphylococcus aureus*

ÖZET

GÜMÜŞ NANOPARTİKÜLLERİN *STAPHYLOCOCCUS AUREUS* BÜYÜMESİ VE α-HEMOLİSİN GEN EKSPRESYONU ÜZERİNDEKİ İNHİBİTÖR AKTİVİTESİ

AI-Hasan Ali Yousif AL-ABAYECHI
Biyoloji, Yüksek Lisans
Tez Danışmanı: Dr. Öğr. Üyesi Zehra CAN KARAHAN
Eş Danışman: Dr. Öğr. Üyesi Meethaq Sattar ABOOD
Aralık 2023

Bu çalışmanın amacı klinik örneklerden *S. aureus* izole etmek, gümüş nanopartiküller sentezlemek ve bunların *S. aureus*'a karşı antibakteriyel aktivitesinin yanı sıra α-hemolizin virülans geninin ekspresyonunu inhibe etme kabiliyetlerini değerlendirmektir. İdrar, yanık ve balgam örnekleri olmak üzere toplam 250 klinik örnek toplandı. *S. aureus* izolatlarını tanımlamak için kültürleme, biyokimyasal testler, API20 testi, Vitek2 sistemi ve PCR kullanıldı. Gümüş nanopartiküller kimyasal indirgeme yöntemiyle sentezlenmiş ve UV-vis spektroskopisi, taramalı elektron mikroskobu (SEM), X-ışını kırınım analizi (XRD) ve Fourier dönüşümlü kızılötesi spektroskopisi (FT-IR) ile karakterize edildi. Antibakteriyel aktivite minimum inhibitör konsantrasyon (MIC), minimum bakterisidal konsantrasyon (MBC) ve agar-kuyu difüzyon deneyi ile ölçüldü. AgNP'lerin α-hemolizin gen ekspresyonu üzerindeki etkisini değerlendirmek için gerçek zamanlı PCR kullanıldı. 250 örnekten 44'ünde (%17,6) *S. aureus* pozitif bulundu. Örnek türleri, cinsiyetler veya yaş grupları arasında izolasyon oranlarında anlamlı bir fark yoktu. AgNP'ler, 14,41 mm'ye kadar inhibisyon zonları ve sırasıyla 8 ve 64 µg/mL MIC ve minimum bakterisidal konsantrasyon değerleri ile iyi antibakteriyel aktivite gösterdi. AgNP'lere maruz kalma, tedavi edilmemiş kontrollere kıyasla *S. aureus* α-hemolizin gen ekspresyonunu önemli ölçüde azaltmıştır. AgNP'lerin virülans faktörlerinin üretimini nasıl etkilediğini bulmak için, nanopartiküllere maruz kalmadan önce ve sonra α-hemolizini kodlayan HLA geninin ekspresyon seviyelerini ölçmek için gerçek zamanlı PCR kullanıldı. Sonuçlar, AgNP'lerin *S. aureus* izolatlarında HLA ekspresyonunu, işlem görmeyen kontrollere kıyasla önemli ölçüde azalttığını gösterdi.Bu da AgNP'lerin antibakteriyel etkilerinin yanı sıra virülansı baskılama kabiliyetine de işaret etmektedir.Son olarak, kimyasal olarak sentezlenen

AgNP'ler klinik *S. aureus* izolatlarına karşı güçlü antibakteriyel ve antivirülans özellikler göstermiştir, bu da ilaç olarak faydalı olabileceklerini göstermektedir. AgNP antibakteriyel ve antivirülans etkisinin kesin mekanizmaları hakkında daha fazla çalışma yapılmasını gerektirmektedir. Genel olarak, bu çalışma AgNP'lerin *S. aureus* enfeksiyonları için bir tedavi yaklaşımı olarak umut vaat ettiğini göstermektedir.

2023, 90 sayfa

Anahtar Kelimeler: Gümüş nanopartiküller, α-Hemolisin geni, *Staphylococcus aureus*

PREFACE AND ACKNOWLEDGEMENTS

To the one who encouraged me to persevere throughout my life To my dear mother, tender heart.

To everyone who contributed even a letter in my academic life.

I extend my thanks to my supervisors, Asst. Prof. Dr. Zehra CAN KARAHAN and Asst. Prof. Dr. Meethaq Sattar ABOOD, and to the discussion committee.

AI-Hasan Ali Yousif AL-ABAYECHI

Çankırı-2023

CONTENTS

LIST OF SYMBOLS

^{o}C	Celsius
ΔCT	Delta Ct corresponds
g/mL	Grams per milliliter
gm	Gram
Θ	Intermediate structure formed during the replication of a circular DNA molecule
µl	Microliter
mm	Millimeter
µg/mL	Micrograms per milliliter
ng	Nanograms
%	Percentage
pmol	Picomoles per liter
Rpm	Revolutions per minute
λ	Wavelength

LIST OF ABBREVIATION

CHIPS	Chemotaxis inhibitory nutrient of *S. aureus*
CoNS	Coagulase-Negative Staphylococci
DLS	Dynamic light scattering
DMSO	Dimethyl sulfoxide
Efb	Extracellular fibrinogen binding protein
Eap	Extracellular rigidly adhering protein
HIV-1	Human immunodeficiency virus-1
H_2O_2	Hydrogen peroxide
JCPDS	Joint Committee on powder diffraction standards
MIC	Minimum inhibitory concentration
MSSA	Methicillin-susceptible *S. aureus*
MRSA	Methicillin-resistant *Staphylococcus aureus*
MgCl2	Magnesium chloride
dNTPs	Nucleoside triphosphates containing deoxyribose
PBS	Phosphate buffer saline
KCl	Potassium chloride
PVP	Polyvinyl pyrrolidone
Ag NPs	Spherical silver nanoparticles
SAK	Staphylokinase
SCIN	Staphylococcal complement inhibitor
SEM	Scanning electron microscopy
GN-GP	The interface between the SGSNs and the GGSNs
SSSS	The staphylococcal scalded skin syndrome
sarA	The staphylococcal accessory regulator)
TEM	Transmission electron microscopy
Tris-HCl	Tris Hydrochloride
FWHM	The full width at half maximum
XRD	X-ray diffraction

LIST OF FIGURES

LIST OF TABLES

1. INTRODUCTION

Numerous species of *Staphylococcus*are both physiologically and pathologically harmful to humans (Gonzalez *et al.* 2020, Fernandes *et al.* 2020). *Staphylococcus aureus* is the most notable and prevalent species. Among the many deadly diseases it may cause is *Staphylococcus aureus*, which is responsible for 18.9 percent of surgical site infections (Sowik *et al.* 2020).

Furthermore, it stands out due to its capacity to produce resistance mechanisms, which might provide challenges to treatment (Cordeiro *et al.* 2020). According to this, the rate of methicillin-resistant *Staphylococcus aureus* (MRSA) that is acquired in hospitals in China is already at 50.4% (Guo *et al.* 2020). After *S. aureus*, *S. epidermidis*is the species of *Staphylococcus* that is found to be isolated the second most commonly (Caballero *et al.* 2021). This bacterium, known as Coagulase-Negative Staphylococci (CoNS), is said to contribute to the microbiota of human skin, mucous membranes, and the respiratory system, as stated by Caballero *et al.* (2021) and Fournière *et al.* (2020).

It accounts for 65–90% of the bacteria found on skin and mucosal membranes, and it causes nosocomial infections such as bacteremia, perioperative infections, and UTIs (Wang *et al.* 2016). Both of these species of staphylococci have been associated with periprosthetic joint infections in patients who have undergone surgical procedures. This is due to the fact that these pathogenic microorganisms have the ability to create biofilm, which is a trait that makes them more resistant to the antibiotic treatment that is currently in use (Koch *et al.* 2020).

To stop *S. aureus* from growing, silver nanoparticles (AgNPs) and a number of antimicrobial drugs have been used. Typically, AgNPs with MIC values of 0.25, 6.25, 12.5 and 50 mM are used for this function. Commonly used are spherical silver nanoparticles (Ag NPs) with a size range of 12–16 nm (Bindhu and Umadevi 2014, Ajitha *et al.* 2014, Lara *et al.* 2010). The next generation of antimicrobials is Ag-NPs. Gram-positive and Gram-negative bacteria, such as *Escherichia coli, Staphylococcus aureus, Bacillussubtilis, Streptococcus mutans, and Staphylococcus epidermidis* are all destroyed

by the antibacterial action of Ag-NPs, which has a very broad spectrum (Lee *et al.* 2008, Jung *et al.* 2008, Yamanaka *et al.* 2005, Espinosa-Cristo´bal *et al.* 2009, Cho *et al.* 2005, Sondi and Salopek-Sondi 2004, Yoon *et al.* 2007, Kim *et al.* 2007). Ag-NPs also strongly stop the growth of *Candida albicans, Candida glabrata, Candida parapsilosis, Candida krusei,* and *Trichophyton mentagrophytes* (Kim *et al.* 2008), as well as human immunodeficiency virus-1 (HIV-1) (Lara *et al.* 2010), *hepatitis B virus* (Lu *et al.* 2008), *herpes simplex* (Baram-Pinto *et al.* 2009), and *monkeypox* (Rogers *et al.* 2008).

Respiratory syncytial viruses are other viruses that Ag-NPs have antiviral efficacy against (Sun *et al.* 2005). Ag-NPs appear to have a notable amount of antibacterial action. In the order shown below, silver is more harmful to microbes than several other metals: Ag, Hg, Cu, Cd, Cr, Pb, Co, Au, Zn, Fe, Mn, Mo, and Sn (Zhao and Stevens 1998). Additionally, compared to silver ions and other silver salts, Ag-NPs are more effective at mediating their antibacterial activity (Lok *et al.* 2006, Rai *et al.* 2009). And compared to many other antibacterial materials, silver has a reduced tendency to cause microbial resistance (Kim *et al.* 2007, Silver 2003, Silver *et al.* 2006, Frankee*t al.* 2001). The wide range of applications for Ag-NPs is mostly due to their antibacterial properties, which help to avoid infections in many settings. Wound bandages for burns and trauma, diabetic ulcers, dental therapies, dental scaffolds, and medical equipment are all part of this category (Rai *et al.* 2009, Law *et al.* 2008, Silver *et al.* 2006, Kim *et al.* 2007, Thomas *et al.* 2007, Kim and Kim 2006).

Additionally, sanitary products, including toilet seats, washing machines, dishwashers, and water filtration systems, use Ag-NPs (Silver *et al.* 2006, Rai *et al.* 2009). It is still unclear how Ag-NPs work as antimicrobials, despite their extensive usage as microbial agents in several goods. The function of gram-positive bacteria, however, is poorly understood. It is plausible that Ag-NPs do not function similarly on Gram-negative and positive bacteria due to the fact that the cell architectures of these two types of bacteria are so different (Silver *et al.* 2006). In this study, we looked at the action mode of Ag-NPs on bacteria using the Gram-positive bacterium *S. aureus*.

Aims of this study

This study aimed to isolate *S. aureus* from clinical samples, synthesize silver nanoparticles, and evaluate their antibacterial activity against *S. aureus*, as well as their ability to inhibit the expression of the α-hemolysin virulence gene.

2. LITERATURE REVIEW

2.1 Pathogenicity and Antimicrobial Resistance of *Staphylococcus aureus*

The biochemical properties of *Staphylococcus aureus* include being catalase and coagulase positive, in addition to being a non-motile, spore-forming, gram-positive, facultative anaerobe. It may be seen growing in pairs or as an unusual cluster resembling grapes; its colonies are often smooth and elevated, and their colour can vary from yellow to golden yellow. The presence of 5% sheep or horse blood in the blood agar causes these colonies to be hemolytic (Turnidge *et al.* 2008, Plata *et al.* 2009). Up to now, scientists have identified over 40 different species of *Staphylococcus*; nine of these species have two subspecies, and one has three. Staphylococci are still in the process of being categorized, and new species that are now going through the validation process are constantly being reported (Doskar *et al.* 2010).

S. aureus is a pathogen that can colonize the skin as well as the mucous membranes of the throat, anterior nasal passages, gastrointestinal tracts, perineum, and genitourinary tracts. It is exceedingly contagious, in addition to being broad and adaptable (den Heijer *et al.* 2013). It is the leading cause of a range of diseases both in humans and animals, and as a result, it has a substantial effect on the state of public health (Luzzago *et al.* 2014). The potential for zoonotic transmission, host specialisation, and the acquisition and loss of virulence and resistance genes have all had major impacts on public health (Holden *et al.* 2004, Saleha and Zunita 2010, Luzzago *et al.* 2014).

From a medical perspective, *staff staph* is the most dangerous staphylococci genus member. Septicaemia, newborn necrotic pneumonia, endocarditis, and superficial skin abscesses are just a few of the many ailments it may cause. It can also cause food poisoning. The majority of food poisoning cases in the US are caused by *Staphylococcus aureus* (Shaw *et al.* 2004). The disease is made worse by genes that make antibiotics less effective. These genes include *mecA, vanA,* staphylococcal exotoxins, and others. They help the disease start, send signals, and damage host tissue. Additional contributors to the severity of the disease are: (Holden *et al.* 2004, Shaw *et al.* 2004). It wasn't until a strain

of *Staphylococcus aureus* developed penicillinase, a hydrolyzing enzyme that made it resistant to penicillin, that antimicrobial resistance in *S. aureus* was first noticed in the mid-1940s. Antibiotic resistance in *Staphylococcus aureus* has never been shown before (Basset *et al.* 2011).

Since then, penicillin-resistant *S. aureus* strains have been frequently identified in bacteremia cases in both the United Kingdom and the United States. Due to the fact that these antibiotic-resistant strains were first discovered in hospitals, the definition "nosocomial associated penicillin resistance *S. aureus*" was used to describe them. Later, it was discovered that a portion of the population carried antibiotic-resistant bacteria that were unrelated to the strains found in hospitals by any obvious risk factors (Chuang and Huang 2013). From the late 1940s to the early 1960s, penicillin resistance increased as a direct result of this. Methicillin, a semisynthetic homologue of amoxicillin, was subsequently introduced as a preferred treatment for *S. aureus* infection. Methicillin was first created in the 1940s (Jevons 1961).

Resistance to methicillin was observed in *S. aureus* less than a year after the drug was introduced as an appropriate strategic treatment for the treatment of bacteraemia. Due to the formation of a genomic island containing the mecA methicillin resistance determinant, methicillin-resistant *S. aureus* (MRSA) has emerged. Since its discovery in the United Kingdom in the early 1960s, multidrug-resistant *S. aureus* has become the leading cause of infections in humans, communities, and livestock worldwide. As a result, the therapeutic efficacy of a substantial number of vitally important antibiotics is diminished, and patients spend more time in the hospital (Purrello *et al.* 2011). Possible explanations for the evolution of MRSA include the maintenance of existing clones and the transformation of methicillin-susceptible *S. aureus* (MSSA) into the current strain. This is a contribution to the discovery of a genotype that confers methicillin resistance. This gene encodes a penicillin-binding enzyme that is resistant to all classes of beta-lactamese antibiotics. The mechanism by which *S. aureus* acquires antibiotic resistance was the primary focus of this review (Noto *et al.* 2008).

2.2 *S. aureus* Virulence Factors

The wide variety of disorders caused by *S. aureus* is associated with its many virulence factors, which allow the bacteria to stick to surfaces, enter or escape the immune response, and cause harm to the host (Lowy 1998, Holmes *et al.* 2005).

2.2.1 Adherence factors (Adhesins)

The colonisation process begins when *S. aureus* attaches to the surface of the host cell via a variety of adhesins. The threonine residue in the sortation signal motif at the C-terminus allows members of one notable family of *S. aureus* adhesins to form a covalent bond with cell lipopolysaccharides, and these adhesins attach selectively to components of the plasma or extracellular matrix. One name for this adhesin is ECM, or type I adhesin (Foster and Hook *et al.* 1998, Speziale *et al.* 2009, Maresso *et al.* 2008, Maresso *et al.* 2008). As a group, these proteins are referred to as the microbial surface elements that recognize sticky molecules (MSCRAMMs). These molecules may be used to identify the key components of the extracellular matrix or blood plasma, including fibrinogen, fibronectin, and collagens (Lowy 1998, Flock *et al.* 1987, Cheung *et al.* 2002).

Plumbing factor (Clf) A and B proteomes, lectin proteins, Staphylococcal Protein A (SpA), and fibroblast proteins A and B (FnbpA and FnbpB) are all members of the MSCRAMM protein family (Lowy 1998, Foster Hook *et al.* 1998).

2.2.2 Exoproteins of *S. aureus*

Enzymes such nucleases, proteases, lipases, hydrolases, and collagenases are among the many exoproteins that most *S. aureus* strains are able to secrete. A small number of these exotoxins are also present. These proteins likely play a function in converting surrounding tissue into nutrients that bacteria need for development (Dinges *et al.* 2000).

The cytolytic effects of *S. aureus* exotoxins are well-documented. By opening up barrel holes in the plasma membrane, cytolytic toxins induce their target cells to lyse and release their contents (Foster 2005). *S. aureus* is capable of producing a number of cytolytic toxins, including leukocidin, Panton-Valentine leukocidin, α-hemolysin, β-hemolysin, and γ-hemolysin. These toxins are classified as PVL (Kaneko *et al.* 2004).

Osmotic cytolysis is brought on by a protein called α-hemolysin, which was introduced into the eukaryotic membrane. This protein subsequently forms a β-barrel, which generates a pore in the membrane. Platelets and monocytes are the two human cell types most vulnerable to its cytotoxicity (Menestrina *et al.* 2001). As a bicomponent cytolysin composed of LukF-PV and LukS-PV, PVL has the potential to traverse the host plasma membrane and puncture it by hetero-oligomerization. However, PVL has a marked bias towards leukocytes, in contrast to other bicomponent poisons such as γ-hemolysin and leukocidin, which are toxic to both types of blood cells (Kaneko *et al.* 2004).

Many different kinds of exotoxins can be made by *S. aureus.* These include enterotoxins (SEA, SEB, SECn, SED, SEE, SEG, SEH, and SEI), toxic shock syndrome toxin-1 (TSST-1), and erythema toxins (ETA and ETB). One of them, known as TSST-1, is a member of the class of toxins known as proinflammatory toxin super antigens, which also includes the staphylococcal endotoxins (PTSAgs) (Lina *et al.* 2004, Holtfreter and Broker 2005).

Staphylococcal bacteria are responsible for producing these toxins. This toxin's ability to make T-lymphocytes multiply is called its superantigenicity, and it is this property that has been studied the most in depth. These toxins are responsible for causing food poisoning in addition to toxic shock syndrome. The staphylococcal toxins ETA and ETB are what because the staphylococcal scalded skin syndrome (SSSS) (Melish and Glasgow 1970). Even though it has been known for a long time that exfoliative toxins have the ability to activate oncogenic activity in T cells (Morlock *et al.* 1980). The question of whether or not they may be termed superantigens is still open for debate.

It has been shown that other *S. aureus* proteins may significantly impact the innate and adaptive immune systems. In this class of proteins you'll find, among other things, Efb, Eap, staphylokinase, CHIPS, and formyl peptide receptor-like-1 antagonist protein. An inhibitor known as SCIN blocks the C3 convertase enzyme, preventing the bacteria from producing C3b on their surface. This prevents *S. aureus* from being consumed by human neutrophils (Rooijakkers *et al.* 2005). Epa prevents neutrophil migration from blood arteries into tissue, whereas CHIPS and FLIPr block neutrophil receptors for chemoattractants (Chavakis *et al.* 2002). SAK binding to defensins eliminates their bactericidal properties (Bokarewa *et al.* 2006), and CHIPS and FLIPr block neutrophil receptors for chemoattractants (De Haas *et al.* 2004, Prat *et al.* 2006) and at the same time Efb (Lee *et al.* 2004).

It is generally accepted that virulence is complex as well as the consequence of the interaction of a large number of different virulence factors. The presence of the toxin that causes toxic shock syndrome, as well as exfoliative toxins A and B, as well as various staphylococcal enterotoxins, is an exception. These toxins are responsible for SSSS, toxin shock syndrome, as well as staphylococcal food poisoning, respectively (Lowy 1998).

S. aureus-induced ventilator-associated pneumonia is associated with a wide variety of virulence variables. *S. aureus* may adhere to the respiratory epithelium, break the project barrier, and draw in PMN due to the actions of LTA, PepG, MSCRAMMs (namely Fnbp and SpA), and toxin. All of these things might happen at the same time (Ferry *et al.* 2008). The cell-damaging SpA, -toxin, and -toxin are also linked to necrotizing pneumonia; they irritate and eventually kill the respiratory epithelium. Death may result from necrotizing pneumonia. It is unclear whether or not PVL has a role in the development of necrotizing pneumonia (Bartlett *et al.* 2008).

2.2.2.1 α-Toxin (α-Hemolysin)

S. aureus is responsible for the release of α-toxin, which is the principal cytotoxic agent. *S. aureus* was the organism that was responsible for the production of this exotoxin, which was the first of its kind to be identified as a pore creator. Membrane permeabilization

causes changes in ion gradients, membrane depletion, activation of stress signalling pathways, and, finally, cell death in vulnerable host cells (Husmann *et al.* 2006).

It is known that *S. aureus* α-toxin is a major factor in the development of staphylococcal diseases because mutants of *S. aureus* that lack HLA have lower virulence in invasive disease models (Wardenburg *et al.* 2008). It's interesting to note that the toxin might operate in two different ways, depending on the dosage. Low amounts create a heptameric pore by binding to particular cell surface receptors. By allowing the interchange of monovalent ions, this hole causes DNA breakage and ultimately apoptosis (Bantel *et al.* 2001). The toxin absorbs non-specifically into the lipid bilayer at high concentrations (Hildebrand *et al.* 1991). And developing significant Ca^{2+}-permissive pores. As a result, there is severe necrosis and other cellular responses that are brought on by the unchecked Ca^{2+} influx (Bantel *et al.* 2001).

It is released from host membranes as a water-soluble monomer that changes shape several times to make a β-barrel structure with six heptamers. The interaction of HLA with a proteinaceous receptor that has not been identified before is essential for structural maturation (Wilke *et al.* 2010).

2.2.3 Regulation of virulence factors in *S. aureus*

Colonisation, avoiding host defence, cell division, and bacterial dispersion are only a few of the many steps in the intricate process of *S. aureus* infection that requires the coordinated expression of several extracellular and cell wall components (Torres *et al.* 2010).

There may be global regulators at work when viruses respond to environmental signals by coordinating the expression of various virulence factors; for instance, producing toxins later in the infection to aid the virus's spread through the tissue vs early expression of adhesins during colonisation. In these regulators, the expression of several unrelated target genes is controlled by a single regulatory component (Cheung *et al.* 2004). These

regulators help bacteria adapt to a harsh environment by making components that let them survive and then cause infection at the right moment.

Most likely to influence the expression of virulence factors are changes in the availability of nutrients, temperature, pH, osmolarity, and oxygen tension, among other environmental cues (Torres *et al.* 2010). Production Several global regulatory loci, such as the accessory gene regulator (AGR), control the factors that determine *s. aureus* pathogenicity (Peng *et al.* 1988), the staphylococcal accessory regulator (*sarA*) (Cheung *et al.*2001), the *sae* (Giraudo *et al.* 1994), the *sigB* (Bischoff *et al.* 2001), and the arl (Fournier Arvidson *et al.* 2001). These regulators are crucial nodes in the network that controls how *Staphylococcus aureus* expresses its pathogenicity genes. Several regulators "cross talk" with each other to regulate the expression of a target virulence gene only when conditions are suitable. The spa gene encodes SpA, and in vitro experiments have shown that agr suppresses its expression, but SarS binds to its promoter and increases spa synthesis (Tegmark *et al.* 2000). It's interesting to note that agr reduces *sarS* expression (Cheung *et al.* 2001, Tegmark *et al.* 2000). Therefore, it has been postulated that agr inhibits the expression of spa's activator, *sarS*, in order to lower spa expression. Thus, virulence gene regulators may regulate the expression of their target genes either directly or indirectly by binding to their promoters (Tegmark *et al.* 2000).

2.3 Silver Nanoparticles

Of all the metallic nanoparticles, AgNPs have the highest potential for use in nanotechnology. Modern nanotechnology research is heavily focused on developing dependable methods for producing AgNPs. The optical, electrical, and magnetic features of AgNPs make them particularly useful for a variety of applications, including antibacterial, antiviral, and antifungal ones. They can also be used in composite fibers, biosensor materials, cosmetic items, the food sector, and electronic components (Senapati *et al.* 2005, Klaus-Joerger *et al.* 2001).

Shampoos, detergents, soaps, toothpaste, and cosmetics are some of the products that have reportedly contained AgNPs as medical and pharmaceutical substances that have

come into direct contact with a human system (Banerjee *et al.* 2014). AgNPs are applied as antibacterial (Sondi *et al.* 2004), antifungal (Kuppusamy *et al.* 2016), anti-inflammatory (Gurunathan *et al.* 2009, Narayanan *et al.* 2014), antiviral (Suriyakalaa *et al.* 2016), anti-inflammatory (Kuppusamy *et al.* 2016), and anti-diabetic medicines in the biomedicine (Olaleye *et al.* 2010). Recent studies have also revealed the use of AgNPs for cancer diagnosis, therapy, and drug delivery using either active or passive processes (Akhtar *et al.* 2013). It has been known that silver possesses antibacterial qualities since ancient times. Nowadays, silver is used to prevent the transmission of germs in several locations, including dental procedures, catheters, and burn sites. It is well known that silver ions and compounds containing silver are very poisonous to bacteria and exhibit potent biocidal properties (Sanghi *et al.* 2009).

AgNPs are mostly used in molecular diagnostics and photonic devices because of their optical characteristics. The usage of AgNPs as antimicrobial coatings is on the rise. It has been known that silver possesses antibacterial qualities since ancient times. Dental procedures, catheters, and burn sites are just a few of the modern situations where silver is utilised to prevent the transmission of germs. The significant biocidal effects of Ag ions and Ag-based compounds on microorganisms are well-known (Sanghi *et al.* 2009). AgNPs are mostly used in molecular diagnostics and photonic devices because of their optical characteristics. AgNPs are being used more and more for antimicrobial coatings (Al-Thabaiti *et al.* 2016).

2.4 AgNPs Synthesis

To create metallic nanoparticles, many techniques classified as bottom-up or top-down procedures are applied (Silva *et al.* 2017). Upper-level approaches produce stable AgNPs via nanoscale synthesis of nanoparticles from solid or aerosolized metallic silver. This class includes physical procedures such as sputtering, laser ablation, and ball milling (Kulkarni *et al.* 2014, Nakamura *et al.* 2011, Jara *et al.* 2015). To make nanoparticles, bottom-up processes include stabilising and nanostructuring silver atoms using several methods. To make nanoparticles, bottom-up methods are used in the chemical and biological sciences (Silva *et al.* 2017, Tran *et al.* 2013).

It is common practice to use physical procedures to create vast quantities of nanoparticles; the level of purity of these particles might vary from process to process. However, the majority of the time, these techniques require expensive equipment, high pressure, and high temperatures (Yaqoob *et al.* 2020, Zhang *et al.* 2016). Chemical methods for producing AgNPs include electrochemical, sol-gel, and chemical reduction procedures. They allow for the production of nanoparticles with a certain spherical shape and are believed to be affordable (Yaqoob *et al.* 2020, Elsupikhe *et al.* 2015, Dang *et al.* 2012).

With only three simple ingredients—a metallic precursor, a reducing agent, and a stabilising agent—these processes are thought of as simple and scalable. Toxic reagents or solvents are often a part of these chemicals, therefore mandating their usage may lead to the production of harmful or polluting waste (Tran *et al.* 2013, Krutyakov *et al.* 2008). The third way of biologically synthesizing nanoparticles comprises all processes utilizing biologically derived materials or living organisms, whether through bacterial or fungal mediation or through the use of natural extracts as reagents (Nam *et al.* 2008, Balaji *et al.* 2009). AgNPs produced biologically have been shown to be highly soluble, yielding, and stable (Chung *et al.* 2016).

The introduction of organisms or reagents of biological origin, however, makes this synthesis more complex and necessitates the use of substances with high stabilizing and reducing agent capacities. However, given its low cost and the range of natural resources that can be employed to reduce the potential toxicity of nanoparticles, this is thought to be one of the most promising technologies (Zhang *et al.* 2016). The methodologies, equipment, and conditions needed for each approach vary, which determines their challenges and comparative advantages. Figure 2.1 lists the synthesis techniques in brief. The size, stability, and biological effects of the nanoparticles, which define their chemical surface and ion release capability, will all be influenced by the synthesis process used. Because of this, the synthesis will determine their biological activity and potential toxicity (Krutyakov *et al.* 2008, Korshed *et al.* 2019).

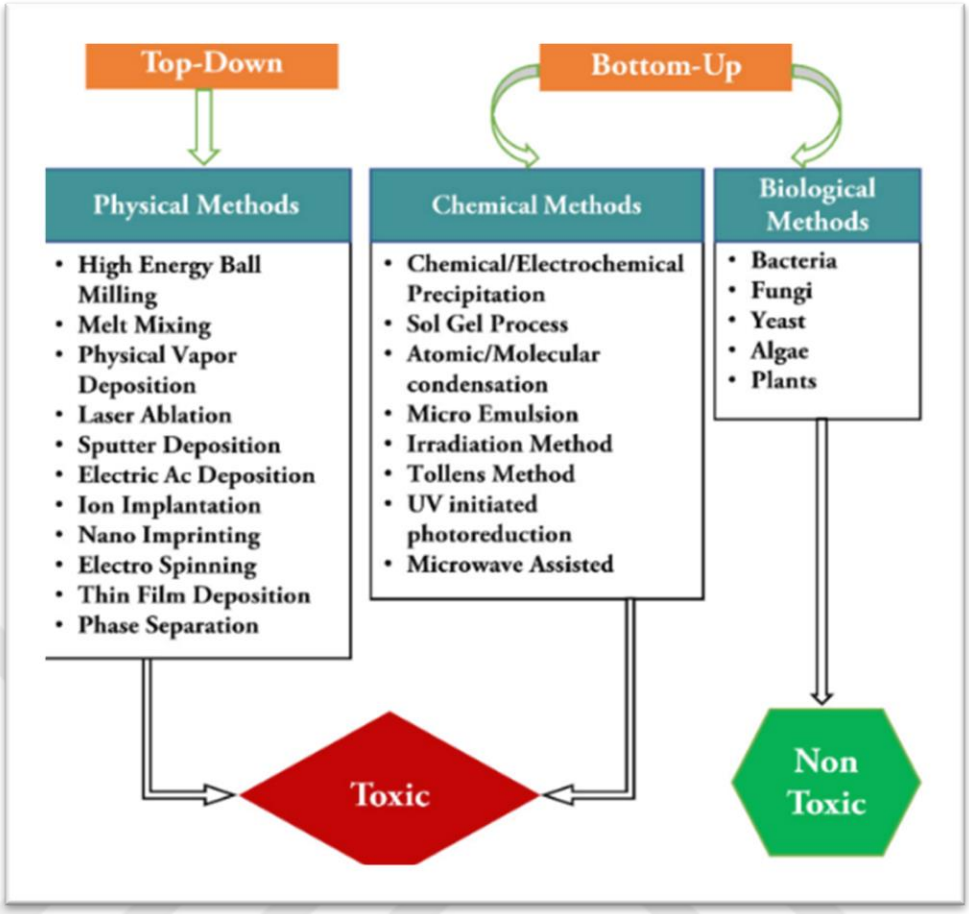

Figure 2.1 Different types of methods used for the synthesis of nanoparticles (Krutyakov *et al.* 2008)

2.5 Nanobiotechnology Related Applications

In order to create metal nanoparticles, scientists use a variety of physical and chemical approaches. These methods for different synthesized chemicals are pricey, though. They could lead to the development of poisonous chemical organism nanoparticles on the surface, which could have negative effects on a variety of biological and medicinal applications (Mittal *et al.* 2014). The demand to create "green synthesis" processes for synthesizing nanoparticles in the environment is growing.

Since AgNPs are one of the most thoroughly studied nanomaterials and the most popular target of the aforementioned "green" approaches, scientists are enamored with them. Research areas and the creation of nanoparticles using plant extract are developing. Metal

nanoparticles can be synthesized inside and outside cells using plant structures (Renugadevi *et al.* 2012). When it comes to processing nanoparticles, hydroponic solutions like metal-rich soils and seed plants grown in high-metal mediums are just two examples. Extract leaves are made from nanoparticles extracted from the leaves by heating or shaping them in water or alcohol (Parashar *et al.* 2009). It was Medicago sativa, the first plant known to have been used to synthesize extracellular nanoparticles, which was used to create silver and gold nanoparticles (Gardea *et al.* 2003).

As a result, the utilization of plants as substrates for the production of nanoparticles has received considerable interest. When it comes to treating wounds and burns and creating nano-containing components for bone replacement and dental materials, AgNPs have been found to be effective antibacterials, antifungals, antiviruses (including *HIV*), anti-protozoans, anti-arthropods (including bedbugs), anti-larvicidals, and anti-cancer agents. AgNO3 was an important antibacterial agent in medicine prior to the introduction of AgNPs (Anjum *et al.* 2016). The use of nanoscale materials in nanotechnology has skyrocketed in the last few years. It will be used in the future to diagnose and stop numerous illnesses in biomedical applications. Titanium or titanium alloys can be used to coat AgNP-coated dental titanium implants (Anjum *et al.* 2016).

2.5.1 Antimicrobial applications

The development of nanotechnology has heightened interest in and understanding of the antibacterial effectiveness of AgNPs. According to a comparison of AgNPs, AgNO3, and AgCl (Choi *et al.* 2008), AgNPs are more effective at killing bacteria than free silver ions. There are a lot of very harmful bacterial species that the AgNPs bactericide has been shown to effectively kill, as well as Gram-positive and Gram-negative bacteria (Anjum *et al.* 2016). In 2007, Kim and his colleagues did an experiment to see how antibacterial AgNPs are. They used *Staphylococcus aureus* and *Escherichia coli* as examples of gram-positive and gram-negative bacteria. The smallest amount of AgNPs needed to stop *S. aureus* from growing is ten times higher than the lowest amount needed to stop *E. coli* from growing (3.3 to 33 nM). Another study found that AgNPs (10–15 nm) were highly effective antibacterial agents and had increased stability when used against various drug-

resistant bacterial strains. Multiple reports indicate that gram-negative bacteria are more susceptible to the dose-dependent antibacterial effect of AgNPs compared to gram-positive bacteria (Kumar *et al.* 2014). The AgNPs also showed promise as an antibacterial agent against gram-positive bacteria like *S. aureus*, which is found in human infections, and gram-negative bacteria like *E. coli* and *Klebsiella pneumonia*, which are resistant to many drugs. Target microorganisms, compound forms, and silver concentration all affect AgNPs' antibacterial behavior (Sadeghi *et al.* 2012, Guzman *et al.* 2011).

A high concentration of silver reagent (AgNO3, AgCl) is required to prevent bacterial cell development. Preventing infections brought on by viruses, bacteria, fungi, and parasites was one of the biggest issues in aquaculture. Antimicrobials have historically been employed in aquaculture to eradicate bacterial illnesses. The therapies are now less effective due to resistant strains brought on by the overuse of these chemicals. Tetracycline was the antibiotic most frequently used, according to a prior study (Tuevljak *et al.* 2016) that examined resistant strains in fish producers across 25 nations. Tetracycline, erythromycin, and streptomycin are just a few of the antibiotics for which the isolated tilapia bacteria exhibit resistance. *Listeria sp., Vibrio sp., Pseudomonas sp., Edwardsiella sp., Photobacterium damselae, Yersinia ruckeri, and Aeromonas salmonicida* were among the resistant strains. To eliminate Vibrio harveyi-infected Feneropenaeus indicus organisms, Camellia sinensis generates AgNPs. In vivo studies showed a 70% reduction in bacterial growth at a concentration of 10 g mL-1 (Vaseeharan *et al.* 2010).

Bacillus subtilis is a non-pathogenic organism used to make nanoparticles. Its ability to kill *V. parahaemolyticus* and *V. harveyi* bacteria was tested on Litopenaeus vannamei that had been infected with them. The results showed that Bacillus subtilis inhibited the growth of both of these pathogens. Nanocompounds had a survival rate of ninety percent, which was significantly higher than the control group, which only had a one percent success rate (Sivaramasamy *et al.* 2016). The parasites Ichthyophthirius multifiliis and Aphanomyces were susceptible to the anti-parasitic and antifungal effects of AgNPs that were coated with starch and then applied in immersion baths (20 minutes) at concentrations of 10 ng of nanoparticles. After three days, the findings demonstrated that

the use of AgNPs did not have any negative impacts on the recovery of the fish. Extensive research has been conducted on the potential for silver nanoparticles to be effective in the prevention and treatment of diseases in aquaculture (Barakat *et al.* 2016).

2.6 Mechanism of the Antibacterial Activity of Silver Nanoparticles

Although the exact mechanism behind the antibacterial properties of AgNPs is not completely known, Figure 2.2 suggests a number of potential antibacterial activities. A key component of AgNPs' efficacy is their capacity to continuously release silver ions, which may be thought of as the mechanism via which bacteria are eliminated (Bapat *et al.* 2018). The cell wall and cell membranes may be attached to by silver ions via electrostatic attraction and affinity for sulphur proteins. The bacterial cell wall might burst in this case because the ions that have attached to the cell wall make the cytoplasmic membrane more permeable (Khorrami *et al.* 2018). Absorption of free metallic ions into cells inhibits adenosine diphosphate (ADP) synthesis, which in turn halts ADP production and may cause reactive oxygen species formation (Ramkumar *et al.* 2017). Responsive oxygen species can be the primary cause of cell membrane breakdown and DNA alteration. Silver ions can interfere with DNA replication, impede cell growth, and even kill microbes if they come into touch with phosphorus and sulfur, which are essential to DNA. As Durán and colleagues (2016) have stated, silver ions have been shown to be effective in blocking the creation of proteins in the cytoplasm by denaturing proteins.

Silver nanoparticles' antimicrobial properties (AgNPs):

1. The Ag+ ions released by AgNPs bind to or diffuse across cell membranes and cytoplasmic vesicles, causing damage to both.
2. The destruction of ribosomes silver ions destroy ribosomes, which halts the process of protein synthesis.
3. The presence of silver ions renders the respiratory enzymes on the cytoplasmic membrane inactive, which stops the generation of adenosine triphosphate (ATP).
4. Membrane disruption may occur due to reactive oxygen species. The formation of reactive oxygen species is a byproduct of electron flow breakdown.

5. Damages DNA replication by attaching to it and stopping cell division. Silver and reactive oxygen species also have this effect. This condition is known as a replication block.
6. Once AgNPs build up in the cell wall's fissures, it causes the membrane to denaturate.
7. Perforation of the cell membrane: AgNPs quickly penetrate the cytoplasmic membrane, allowing the liberation of cellular organelles.

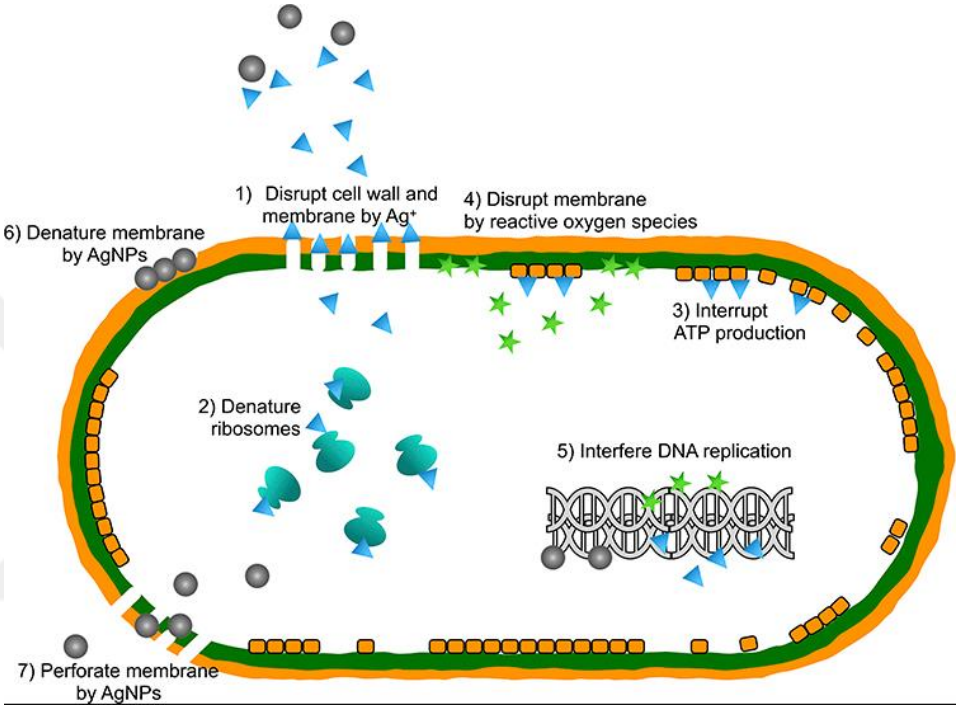

Figure 2.2 Mechanism of silver nanoparticles (AgNPs) antibacterial activity

In addition to releasing silver ions, (AgNPs) may destroy pathogens on their own. Silver nanoparticles (AgNPs) may assemble in cell wall pits after they have attached to the surface of the cell (Liao *et al.* 2019). Cell membrane denaturation may occur if AgNPs were to accumulate. The very small size of silver nanoparticles makes it possible for them to alter the structure of bacterial cell membranes and even enter their cell walls (Liao *et al.* 2019). Organelles might be torn apart and cell lysis could result from cytoplasmic membrane denaturation. Bacterial signal transmission may also include silver nanoparticles. Tyrosine residues on peptide substrates may be dephosphorylated by nanoparticles, and bacterial signalling is affected by protein substrate phosphorylation. Damage to signal transduction pathways may cause cells to die off and stop dividing (Li *et al.* 2019).

How effective silver nanoparticles are against bacteria depends critically on how much of them have dissolved in the exposure medium. The efficiency with which silver nanoparticles dissolve is influenced by both their inherent qualities and the solution in which they are disseminated (Noronha *et al.* 2017). Particle shape and size impact the amount of silver ions released, and the Ostwald-Freundlich equation provides a theoretical explanation for this. Silver nanoparticles with a smaller, more spherical or quasi-spherical shape have a higher surface area and so release more silver (Shanmuganathan *et al.* 2018).

This is also the reason why, according to Noronha *et al.* (2017), aggregated nanoparticles do not emit as much silver as isolated nanoparticles. The solubility of silver nanoparticles may be changed by adding capping agents to their surfaces (Khorrami *et al.* 2018). The release of silver ions is influenced by both the nanoparticles' intrinsic properties and the surrounding environment. Silver nanoparticles' solubility may be affected by organic or inorganic substances in the medium, either by aggregating with them or by complexing with silver ions. Furthermore, research has shown that acidic solutions accelerate the release of silver ions from silver nanoparticles compared to neutral ones (Jacob *et al.* 2019).

Meikle *et al.* (2020) found that silver nanoparticles work better against gram-negative bacteria. Bacteria that are gram-negative have much thinner cell walls than bacteria that are gram-positive. One possible barrier that nanoparticles face while trying to enter cells is the robust cellular membrane. Bacteria need to take up silver nanoparticles for them to kill gram-positive and gram-negative bacteria in distinct ways (Noronha *et al.* 2017). Research has shown that pathogenic bacteria may be infected by silver nanoparticles as small as 10 nm, which can directly affect cell permeability and induce cell damage.

Rapid biofilm formation in the mouth protects bacteria against silver ions and nanoparticles by blocking their mobility. Scientists found that biofilm bacteria did not die off entirely when exposed to silver nanoparticles, even though the same dosage killed all planktonic bacteria (Saravanan *et al.* 2020). Because of its complex structure, the biofilm may tolerate the presence of silver nanoparticles. Size and physicochemical qualities are

common predictors of diffusion coefficients, which in turn affect the mobility and bioavailability of silver nanoparticles in biofilm. It becomes more challenging for larger silver nanoparticles to enter biofilm due to the fact that these parameters diminish with increasing molar mass (Yin *et al.* 2019). Any particle bigger than 50 nm has the potential to greatly impede biofilm movement. Second, nanoparticles' chemical composition may make them adsorb to biofilm, where they would then concentrate and reduce diffusion. Furthermore, the ability of charged nanoparticles to penetrate biofilm may be affected by the electrostatic interaction between bacteria and silver nanoparticles (Pugazhendhi *et al.* 2018).

2.7 Properties of Nanoparticles

Numerous factors affecting the various efficacies of the applied preparations influence the antibacterial activity of nanosilver. Without a doubt, the form of the nanoparticles used has a major impact. According to a substantial amount of study, the form of silver nanoparticles determines their activity. Research has shown that nanoparticles of silver with sharp peaks and edges, which are around 20 nm in size, are more effective in killing bacteria than their spherical counterparts of the same dimension (Tanvir *et al.* 2017). Additional evidence for this result came from a research conducted by Pal *et al.* (2007).

The authors also asserted that compared to spherical particles, prismatic ones exhibit higher reactivity. Prisms with a greater atomic density were postulated by both groups as a possible explanation for this diversity. Additionally, it is contended that the prismatic shapes' planes can experience reduced surface tension. The results demonstrated that compared to spherical or rod-shaped nanoparticles, truncated ones exhibited a higher level of reactivity (Pal *et al.* 2007).

Alshareef *et al.* (2017) found that the effectiveness of nanosilver against bacteria was modified by its shape. Scientific evidence suggests that truncated octahedral nanoparticles may kill *E. coli* bacteria. Bacteriostatic activity was shown by the nanosilver spheres. Geometrically structured nanoparticles with a higher surface area and surface energy may have been more effective in killing bacteria than spherical

nanoparticles (Alshareef *et al.* 2017, Jeevanandam *et al.* 2022). El Zahry *et al.* (2015) found that hexagonal silver nanoparticles were more dangerous than their spherical and triangular counterparts with rounded edges (Table 2.1). The assertions state that this occurred because of its potent penetrating capabilities, which led to cell death in the bacterium (Alshareef *et al.* 2017).

Table 2.1 Different AgNP forms have antibacterial action (El Zahry *et al.* 2015)

AgNPs	**PEG AgNPs**	**Citrate AgNPs**	**Borohydride AgNPs**	**Deionized H2O (Negative Control)**
form	hexagonal	spheral	triple	/
Inhibition zone size (cm) ±SD	2.45 ± 0.24	2.02 ± 0.55	0.08 ± 0.14	0.00 ± 0.00

PEG (Polyethylene Glycol)

Furthermore, the antibacterial effectiveness was concentration dependent for the silver nanoparticles. Platania *et al.* (2021) discovered more nanosilver with a specific particle size, but less *S. aureus* and S. epidermidis. Further research has shown that silver nanoparticles, when mixed with other chemicals like tryptophan, might have an even greater antibacterial effect than when used alone (Leng *et al.* 2020; Courrol *et al.* 2019). Leng *et al.* (2020) found that compared to using the nanoparticles alone, combining them with zinc yielded better results. Coating silver nanoparticles with poly-L-arginine improved their cell-cell interaction in a separate research (Tanvir *et al.* 2017). The combination of tobramycin with silver nanoparticles ranging in size from 10 to 60 nm was also shown to be more effective (Habash *et al.* 2017). This is in line with the findings, which demonstrate that sulfonamides have a negative effect on the effectiveness of silver nanoparticles when used with quorum sensing inhibitors (Haiyan *et al.* 2019). These results lend credence to the theory that antibiotics combined with AgNPs increase their effectiveness (Haiyan *et al.* 2019).

3. MATERIALS AND METHOD

3.1 Instruments and Equipments

Table 3.1 displays the tools and equipments that were used throughout the research.

Table 3.1 Instrument and equipments used throughout the study

No	Equipments and tools	Company (Origin)	Country
1	Autoclave	Gallenkamp	England
2	Distillator	Gallenkamp	England
3	Electrophoresis	CBS,scientific	USA
4	Electric balance	Sartorius	Germeny
5	Gradient PCR	Tech.net 500	USA
6	Hot air oven	Gallenkamp	England
7	Hot plate	LKB	Japan
8	Incubator	Gallenkamp	England
9	Sensitive balance	Mettler	Germeny
10	Spectrophotometer	Hetachi	Japan
11	UV-Transiluminator	UVP	USA
12	Transport swab	LKB	USA
13	Centrifuge	Elite-Medichem	India
14	Digital autoclave	Hirayama	Korae
15	Digital camera	Sony	Japan
16	Vortex Mixer	Labcoo	Japan
17	Water bath	Gallenkamp	Japan
18	Refrigerater	Qean	Egypt
19	UV.transmission	Biosan	Germany
20	Micropipate	Gallenkamp	Japan
21	Loop srander	India	Himedia
22	Light microscope	Olympus	Japan
23	Laminar airflow cabinet	K and K Scientific Supplier	Korea
24	Bansen burner	Naugra	India
25	Petri-dish	Labsays	India
26	Electric oven	Binder	Germany
27	Syringe 1ml, 5ml, 10ml	BD Emerald	Spain
28	Shaker water bath	GFI	USA
29	Disposable micropipette tip	Samix	China
30	Disposable Pasteur pipette	Samix	China
31	Eppendrof centrifuge	Bioneer	Korea
32	Microspin	Biosan	Lativa
33	Vitek 2compact	Bio merieux	France
34	Mini vortex	Fisher Scientific	USA
35	PCR thermal cycle system	Thermo	USA
36	AURA TM PCR Cabinet	Italy	Italy
37	Microspin 12,High-speed Mini-centrifuge	Bioan	Germany
38	V-1plu,personal Vortex for tubes	Digsystem	Germany
39	Bio TDB-100, Dry block thermostatbuilt	Biosan	Germany
40	Mini-Power Supply 300V, 2200V	Gosonic	Chain
41	Multigene Optimax Gradient Thermal Cycler	Gosonic	Chain

3.2 Chemical and Biological Materials

Chemicals, reagents, solutions and dyes used throughout the study is shown in Table 3.2.

Table 3.2 Chemicals, reagents, solutions and dyes used in the laboratory experiment

NO	Chemicals	Company	Country
1	Silver nitrate	BDH	England
2	Antiseptic,Disinfectant	Protective No.1	Chain
3	Catalase reagent	BDH	England
4	Bromothymol Blue	Himedia	India
6	Glycerol	Fluka	France
8	Hydrogen Peroxide	BDH	UK
10	Gram stain	BDH	BDH
11	McFarland tubes	Bio-merieux	France
13	Methanol	Fluka	Switzerland
14	NaCl2	BDH	UK
15	Normal Saline (Sterile)	PSI	Saudi
16	Agarose	Conda	USA
17	Red safe staining souluion	Intron	Korea
18	6X Loading dye	Intron	Korea
19	Ladder 100 bp	Intron	Korea
20	Ladder 50 plus	Intron	Korea
21	Premix pcr	Intron	Korea
22	TBE buffer 10 X	Conda	USA
23	Primer	Integrated DNA technologies	USA
24	Bacterial DNA MiniPrep	ZYMO	USA

Cultures Media used throughout the (In-vitro) study is shown in Table 3.3.

Table 3.3 Cultures Media used in the (In-vitro) Study

NO	Name	Company	Country
1	Blood agar base	Biolife	Italy
2	Brain heart infusion agar	Mast diagnostic	England
3	Brain-heart infusion broth (BHIB)	Hi-Medi	India
4	Motility Test Medium	Himedia	India
5	Nutrient agar (NA)	Biolife	USA
6	Muller-Hinton agar	Hi-Media	Italy
7	Nutrient broth (NB)	Difco	England
8	nutrient broth	Himedia	India
9	Urea agar base	Himedia	India
10	Transporte media	Himedia	India

3.3 Preparation of Chemical Solutions

3.3.1 Phosphate buffer saline (PBS, pH: 7.2)

PBS was prepared according to the supplier's instructions by dissolving 8.5 g of NaCl, 1.15 g of Na_2HPO_4, 0.2 g of KH2HPO4 and 0.2 g of KCl in 1 liter of distilled water (Markey *et al.* 2015).

3.3.2 Normal saline

Storing the sterile combination of 8.5 g of NaCl and 1000 ml of distilled water at 4 °C until required, it was autoclaved at 121°C (15 pounds/inch2) for 15 minutes (Markey*et al.* 2015).

3.3.3 McFarland turbidity standards tubes

The turbidity standard [McFarland solution (No. 0.5)] was a ready-to-use solution manufactured by the Bio-Merieux company. Before being transferred to sterile Petri plates or tubes, all media were autoclaved at 121°C (15 pounds/inch2) for 15 minutes after being prepared according to the manufacturer's instructions. After that, they were allowed to harden at room temperature. Sterilisation was achieved by incubating the petri dishes at 37°C for 24 hours. Certain mediums need unique ingredients. In the subsequent steps, they were prepared for bacterial isolation or stored at 4 °C.

3.4 Preparation of Agar Medium

3.4.1 MacConkey agar medium

Following the manufacturer's directions, 51.53 grammes of agar powder were dissolved in 1000 millilitres of distilled water to make it. After dissolving the powder, the mixture was autoclaved and cooled to 50 °C. It was then pipetted onto sterile petri dishes and

placed in the refrigerator at 4 °C. The capacity to detect gram-negative bacteria's fermentation of lactose and to isolate and identify them were its most important uses.

3.4.2 Blood agar medium

Autoclaving was the last step in the preparation process after liquifying 40 g of blood agar foundation powder in 1 litre of distilled water. The mixture was then heated to boiling while stirring frequently to dissolve the medium. After the medium was chilled to 50 °C, 7% sterile sheep blood was aseptically added to it. After making sure the mixture was consistent, the next step was to pour it into sterile petri dishes and stir well. After that, it was allowed to cool to room temperature. After being incubated at 37°C for 24 hours, the petri dishes were deemed sterile. After sterilisation, they were either utilised right away or kept at 4°C until further use in bacterial isolation.

3.4.3 Nutrient agar medium

A litre of distilled water was used to dissolve 28 grammes of nourishing agar powder. After that, the mixture was autoclaved and heated to 50 °C by boiling with frequent stirring. It was then let to settle to room temperature until solid after being placed into sterilised petri dishes. The petri dishes were incubated at 37°C for 24 hours to achieve sterilisation. Either utilise them right away for bacterial isolation or keep them at 4 °C for later.

3.4.4 Brain- heart infusion broth (BHIB)

The recipe called for 37 grammes of BHIB powder to be dissolved in 1 litre of distilled water after being let to sit for about 10 minutes. The medium was dissolved by heating it to boiling and stirring it frequently. After that, the mixture was transferred to autoclaved sterile test tubes. To guarantee sterilisation, the tubes were kept in an incubator at 37°C for 24 hours.

3.4.5 Nutrient broth

Autoclaving was the last step in preparing it after dissolving 13 grammes of nutritional broth in 1000 millilitres of distilled water and adjusting the pH to 7.2.

3.4.6 Mueller-hinton agar

The preparation included combining 1 litre of distilled water with 38 grammes of Muller-Hinton agar powder, heating the mixture to boiling while stirring frequently, and then autoclaving it. After cooling to 50 °C, it was placed onto sterile petri dishes and allowed to settle at room temperature. Before being used for assessing bacteria's sensitivity to antimicrobials, the petri dishes were sterilised by incubating them at 37°C for 24 hours.

3.4.7 Urea agar

To dissolve the autoclaved medium, dissolve 24.01 grammes in 950 ml of distilled water. Bring to a boil, add 50 ml of 40% urea, and allow cool to 50 °C. Pour the mixture in a slanted pattern.

3.5 Samples Collection

Between June 2022 and November 2022, a total of 250 samples were collected at Teaching Al-Hussein Hospital and Al-Nasiriyah General Hospital, including 125 urine, 75 burns, and 50 sputum. A sterile container and swab contained Cary Blair transported media.

3.6 Culture Examination

All specimens were cultured by blood ager and MacConky ager under aseptic technique and then incubated under aerobic conditions at 37 °C for 24-48 hrs. Morphological and biochemical characteristics of a pure colony after growth are important for distinguishing

various types of bacteria (Khan *et al.* 2011). Inspection of pure colony growth, morphology, size, and hemolysis ability on blood ager and lactose fermentation on MacConkey agar, as seen in Figure 3.1.

Figure 3.1 Culture examination by the researcher

3.7 Gram Stain

According to Talaiekhozani *et al.* (2015), gram staining was performed to differentiate the bacterial features and staining ability using a light microscope under an oil immersion lens (ALjanaby and ALhasani 2016).

3.8 Biochemical Tests

3.8.1 Catalase test

The agar medium was separated from the top of the colonies by a loop full of bacterialgrowth. A clean microscope slide is put on the bacterial cells, and a reduction of 3% H_2O_2 has been applied (Quinn *et al.* 2004).

3.8.2 Oxidase test

In a petri dish, a wooden stick and filter paper were used to wet the 1% aqueous solution of tetramethyl-p-phenylenediamine dihydrochloride. The test bacterium is streaked strongly across the filter paper (Quinn *et al.* 2004).

3.8.3 Urease test

By striking, slants of urea agar were injected with fresh colonies and incubated for 24-48 hours at 37 °C, resulting in a change of the agar color from yellow to pink, indicating a positive result (Forbes *et al.* 2016).

3.8.4 Coagulase test

Fibrinogen is transformed into fibrin plasma by the coagulase enzyme. To conduct the reaction, a test tube is filled with 0.1 mL of the tested bacterial isolate and 0.5 mL of citrated plasma solution. The mixture is then incubated at 37 ^{o}C. The tubes are checked for coagulation at half an hour, one, two, and four hours. Positive results are indicated by the formation of a clot within four hours.

3.9 Analytical Profile Index Staph (API Staph) System Confirmatory Tests

There are twenty microtubes in the API Staph Strip, and they hold dehydrated substrates. The tests are reconstituted by inoculating the microtubes with a bacterial solution and preparing them in API Staph Medium. Metabolism causes incubation-related colour changes that may be either detected naturally or brought to light by adding reagents. Read the responses according to the reading table, read the reactions according to the reading table, and then use the Analytical Profile Index or the identification programme to get the identification. An established method for detecting Staphylococcus species, the API staph system categorises bacteria in accordance with the guidelines provided by Biomerieux (Table 3.4).

Table 3.4 Interpretation reading of biochemical test results (API staph)

Tests	ACTIVE INGREDIETS	QTY (mg/cup.)	REACTIONS/ENZYMES	RESULT	
				negative	poistive
0	No substrate		Negative control	red	---
GLU FRU MNE MAL LAC TRE MAN XLT MEL	D-glucose D-fructose D-mannose D-maltose D-lactose(bovine origin) D-trehalose D-mannitol Xylitol D-melibiose	1.56 1.4 1.4 1.4 1.4 1.32 1.35 1.4 1.32	Positive control)(D-GLUcose) acidification (D-FRUctose) acidification (D-ManNosE) acidification (MALtose) acidification (LACtose) acidification (D-TREhalose) acidification (D-MANnitol) acidification (XyLiTol) acidification (D-MELibiose)	red	yellow
NIT	potassium nitrate	0.08	Reduction of NITrates to nitrites	Colorless-light pink	red
PAL	ß-naphthyl phosphate	0.024	ALkaline Phosphatase	yellow	violet
VP	sodium pyruvate	1.904	Acetyl-methyl-carbinol production (Voges Proskauer)	Colorless-light pink	violetpink
RAF XYL SAC MDG NAG	D-raffinos D-xylose) D-saccharose (sucrose) methylαDglucopyranoside N-acetyl-glucosamine	1.56 1.4 1.32 1.28	acidification (RAFfinose) acidification (XYLose) acidification (SACcharose) acidification (Methyl-αDGlucopyranoside) acidification (AcetylGlucosamine)	red	yellow
ADH	L-arginine	1.904	Arginine DiHydrolase	yellow	orange red
URE	Urea t	0.76	URE urea	yellow	redviolet

3.10 Diagnosis of Bacteria by Vitek2 Compact

The bacterial isolates were diagnosed by the integrated VITIC device according to the manufacturer's instructions using GN-GP cards as follows:

1- Suspending the microbe in 3.0 ml of sterile saline requires transferring enough colonies of a pure culture using a sterile swab or applicator stick.
2- The DensiChek turbidity metre is used to standardise the turbidity by comparing it to a 0.5 normal McFarland solution.
3- An integrated vacuum equipment is used to inoculate identification cards with suspensions of microorganisms. The test tube containing the suspension of microorganisms is placed on a designated rack (cassette) prior to inserting the transfer

tube into the appropriate suspension tube. Subsequently, the matching slot is used to insert the identity card. With a cassette that can carry ten tests, the organism suspension is transferred into each well via micro-channels filled with the transfer tube.

4- Before the card is loaded into the carousel incubator, a device shuts the transfer tube after passing it through infected cards.
5- The optical system is used to read reaction readings from incubation cards.
6- By using various visible-light wavelengths, a transmittance optical system enables the interpretation of test responses. The turbidity or coloured results of substrate metabolism may be measured by reading each test reaction every 15 minutes while they are incubating. On top of that, any potential tiny bubbles are eliminated from the measurements by use of a specialised algorithm.
7- Each test's response is determined by doing calculations on raw data and comparing it to thresholds. Positive, negative, and weak responses are shown on the VITEK 2 Compact as test results.
8- The VITEK 2 identification products' databases are built using big strain sets of microbes that have been well-characterized and tested in different culture settings. A wide range of clinical and industrial sources were used to develop these strains.

3.11 Bacterial Isolates Preservation

According to Azizi *et al.* (2014), preservation of isolated bacteria was carried out either by cultured on nutrient and brain heart infusion agar, incubated at appropriate, then stored in the refrigerator at 4 °C and re-cultured monthly for surviving bacteria, or for prolonged preservation by inoculation of bacteria in maintenance broth media supplied with 15% glycerol, then stored at -20 °C.

3.12 Molecular Study

3.12.1 Genomic DNA extraction

After preparation of the bacterial suspension of *S. aureus* isolates, centrifugation (5000 rpm for 10 minutes) was done, then the supernatant was removed completely and the pellet was subjected to DNA extraction according to Integrated DNA Technologies (Genomic DNA Mini Kit):

- For three minutes, the pellet samples were spun at 8,000 revolutions per minute.
- The particle was kept separate from the supernatant during disposal.
- The pellet was mixed with 200 µl of lysozyme using a vortexing motion, and then left to incubate at 37 °C for 1 hour.
- Two hundred microliters of buffer LB1 and twenty microliters of proteinase K were added to the mixture for every sample.
- Prior to the lysis stage, the mixture was vortexed and left to incubate at 60 °C for 15 minutes.
- To the mixture, 200 µl of 100% ethanol was added and stirred using a vortex mixer.
- During the binding process, the mixture was spun on a column at 8,000 revolutions per minute.
- A fresh collecting tube is used to house the spin column after the liquid flow-through is discarded with the old one.
- Next, 500 µl of buffer AW2 was added to the spin column after washing it, and the combination was centrifuged at 8,000 rpm for 1 minute (to complete wash step 1).
- A new collection was made by discarding the collecting tube and spin-placed column together with the liquid flow-through.
- Before being centrifuged at 8,000 rpm for 1 minute during wash step 2, the spin column was washed twice with 500 µl of buffer AW2.
- The liquid flow-through was centrifuged at 12,500 rpm after disposing of the collection tube, spin-placed column, and liquid flow-through in a fresh collection.
- All of the liquid that had flowed through the collecting tube and beneath the spin column ended up in the medical waste bin.
- After positioning the spin column in a sterile 1.5 ml microcentrifuge tube, the ethanol was allowed to evaporate for one minute.
- Before centrifugation at 12,000 rpm for 1 minute, 50-100 µl of buffer EL3 was poured to the spin column and let to sit for 5 minutes (the elution step).

- The DNA sample was contained in the liquid flow-through. Keep the DNA at 4 degrees Celsius for immediate usage or at -20 degrees Celsius for future reference.

3.12.2 Estimation of the extracted DNA concentration and purity

To ensure the DNA was pure, the absorbance at 260/280 nm was read, and a nanodrop spectrophotometer was used to determine the DNA concentration (ng/µL).

3.12.3 Preparing of the primers suspension

In accordance with the manufacturer's instructions, the lyophilized product primers were dissolved to re-suspend the primers, and the stocked primer was made by adding PCR water (free nuclease water). Afterwards, 10 µl of stock primer was diluted with 90 µl of PCR water to make 10 pmol/µl of working primer, which was then well mixed using the vortex.

3.12.4 Polymerase chain reaction (PCR) assays

Table 3.4 shows the components of the PCR that were utilised (Maxime PCR Abm Kit). The procedure was carried out according to the instructions provided by the business. Taq DNA polymerase, deoxyribonucleotides (dNTPs), Tris-HCl pH:9.0, potassium chloride (KCl), magnesium chloride (MgCl2), and loading dye were among the many components needed for the PCR process that were added to standard Maxime PCR Pre Mixtubes, as shown in Table 3.5. After that, each PCR tube was placed in a PCR thermocycler (ABM Canada) and spun at 3000 rpm for 1 minute in an Exispin vortex centrifuge.

Table 3.5 Components of the PCR mixture

PCR mixture	V**olum**e
DNA template	5 µl

Forward primer (10pmol/µL)	3 µl
Reveres primer (10pmol/µL)	3 µl
PCR water	14 µl
Master mix	25 µl
Total volume	50 µl

3.12.5 Polymerase chain reaction (PCR) thermo cycling conditions

The thermal cycler was used to position the PCR tubes, as shown in Table 3.6. Then, depending on the specifics of the experiment, the PCR cycling software was modified for each primer in both conventional and multiplex PCR.

Table 3.6 Programs of multiplex PCR for genes

Genes	Step	Temperature	Time	Cycle
αhimolysin	Initial denaturation	95.0 ^{0}C	5 min.	1
	Denaturation	94.0 ^{o}C	1 min.	30
	Annealing	55.0 ^{o}C	42 sec.	
	Extension	72.0 ^{o}C	40 sec.	
	Final Extension	72.0 ^{o}C	10 mins	1
	Hold	4.0 ^{o}C	Forever	

3.12.6 Agarose gel electrophoresis

Using agarose gel electrophoresis, the PCR products were examined in accordance with the manufacturer's instructions (Plus Science, UK). Following the instructions of Sambrook and Russell (2001), this procedure was executed in the following way:

1- To get a final concentration of 10x (90 ml of distilled water + 10 ml of TBE), 1.5 grammes of agar was added to 100 millilitres of Tris/Borate/EDTA.
2- Bethidium bromide, at a concentration of 0.05 mg/ml, was added to the cooled Tris-borate-EDTA after it had boiled.
3- After pouring the agarose into an equilibrated gel tray, it was let to cool and solidify.
4- The agarose gel wells were filled with five microliters of PCR product, and one of the wells was then used to place DNA markers. After positioning the gel in the

electrophoresis chamber, TBE buffer was introduced to the apparatus. For eighty minutes, an electric current of 70 volts was applied. On a 1.5% agarose gel, the PCR products were found.

5- Lastly, the gel documentation system was used to identify the electrophoresis result. When the sample's DNA band base pairs were the same size as the intended product size, it was confirmed that the findings were positive.

3.12.7 Molecular determination of housekeeping gene and target gene

3.12.7.1 RNA extraction

The extraction of RNA from bacterial cells was performed using a TRIzol kit and in accordance with the manufacturer's protocols, as follows:

1- A loop full of *Staphylococcus aureus* overnight growth was inoculated in 5 ml of nutrient broth and incubated at 37°C for 24 hours.
2- Centrifugation of the bacterial growth at 12.000 rpm for 10 min.
3- Discard the supernatant without touching the pellet.
4- Add 1 ml of the TRIZOL reagent and spin the pellet at 12.000 rpm for 5 min. Lyse cells with the TRIZOL reagent by repetitive pipetting.
5- Add 200 µl of chloroform, vortex for 15 sec., and incubate for 5 min. in the refrigerator.
6- Centrifugation at 12.000 rpm (by cool centrifuge) for 15 min. at 4 °C
7- Transfer the supernatant to a new tube and add an equal volume of isopropanol to it.
8- Mixing the sample vigorously for 4-5 times.
9- Incubate the mixture in the freezer for 10 minutes.
10- Centrifuge the mixture at 12.000 rpm for 10 minutes, then transfer the upper aqueous phase carefully without disturbing the interphase into a fresh tube.
11- Add 1 ml of 80% ethanol.
12- Centrifuge the mixture (12.000 rpm for 10 min), then remove the upper layer.
13- Dry the pellet, then add the free nuclease water for dissolution.

3.13 Real Time-quantitative Polymerase Chain Reaction

3.13.1 Reverse transcriptase (cDNA synthesis) using PCR technique

A master amplification reaction (ABM, Canada) was used for cDNA synthesis and amplification. The following components are mixed to create a 20 µL reaction solution for RT-qPCR:

1. 1.0 µL of forward (F) primer.
2. 1.0 µL of reverse (R) primer.
3. 10 µL of qPCR Master Mix Buffer (2X), (concentration: 1X).
4. 0.4 µL of RT Mix Buffer (50X), (concentration: 1X).
5. 5.6 µL nuclease-free H_2O.
6. 2.0 µL of extracted RNA template.

To determine the cycle threshold (CT) value, the produced solution was subjected to a heat reaction in a real-time PCR cycler. A cycle procedure was carried out as followsas shown in Table 3.7.

Table 3.7 Master amplification reaction component, concentration and volume

No.	Component	Concentration	Volume
1	Nuclease-free water up to 20 µl	-	5.6 µl
2	Bright Green qPCR Master Mix	1X	10µl
3	Forward Primer (6 µM)	300 NM	1 µl
4	Reverse Primer (6 µM)	300 NM	1 µl
5	qRT PCR enzyme Mix (50X)	1X	0.4 µl
6	Total RNA	2pg – 0.2 µg 0.01 pg – 2 ng	2 µl

We used a sure cycler to carry out the thermal cycling response. By finding the optimal temperature that produced the desired band result, the PCR process was optimised. Following the protocol in Table 3.7, the PCR reaction was conducted.

3.14 Real time Polymerase Chain Reaction (PCR) Amplification

3.14.1 Preparing primers suspension of housekeeping gene (GyrA) and target gene (alph-hemol)

The oligonucleotide primers were made into a stock solution by resolving the lyophilized product with nuclease-free water after a short spinning down, following the manufacturer's instructions.

180 µLnuclease-free water

F-GyrA-aureus

5-ATTGCAGAGCTCGTTCGTGA-3

R-GyrA-aureus

5- ATAACGACACGCACACCAGT-3

F-alph-hemol-aureus

5-TGGTTTAGCCTGGCCTTCAG-3

R-alph-hemol-aureus

5- GCACCAATCAAACCGCCAAT 3

Table 3.8 PCR program and cycling protocol

No.	**Step**	**Temperature**	**Duration**	**Cycle**
1	cDNA synthesis	42 ºC	15mins	1
2	Pre – denaturation	95 ºC	10 mins	1
3	Denaturation	95ºC	15sec	40
4	Annealing	60 ºC	60sec	40
5	Melt curve	According to the instrument guidelines		

Gene expression levels may be measured using real-time polymerase chain reaction (RT-PCR). These measures are computed from the recorded CT readings taken during the heat response (Abtan 2017).

3.14.2 Data analysis of qRT-PCR

We used the Livak approach, as described by Livak and Schmittgen (Livak and Schmittgen 2001), to ascertain the expression level (fold change) of every gene. In order for the results of the q RT-PCR experiment to have any biological significance, it is necessary to standardise both the relative quantification approach and the amounts acquired. The control samples or another experimental sample serves as a calibrator in this approach. Divide all of the CT values by the calibrator's normalised target value to obtain the relative expression levels as shown in Table 3.9. Following that, the protocols for using the ΔCT Method using a Reference Gene were as follows:

$\Delta CT\ (calibrator) = CT\ (target, calibrator) - CT\ (ref, calibrator)$

$Ratio\ (target / reference) = 2^{CT\ (reference) - CT\ (target)}$

Table 3.9 CT values required for relative quantification with reference gene

	Test	**Calibrator (cal)**
Target gene	CT(target, test)	CT(target, cal)
Reference gene	CT(ref, test)	CT(ref, cal)

First, normalize the CT of the reference (ref) gene to that of the target gene for the calibrator sample.

Second, normalize the CT of the reference (ref) gene to that of the target gene for the test sample.

$\Delta CT\ (Test) = CT\ (target, test) - CT\ (ref, test)$

$\Delta\Delta CT = \Delta CT\ (test) - \Delta CT\ (calibrator)$

Fold change = $2^{-\Delta\Delta CT}$

Ratio (reference/target) = $2^{CT\ (reference) - CT\ (target)}$

So, the relative expression was divided by the expression value of a chosen calibrator for each expression ratio of the test sample.

3.15 Synthesis of Silver Nanoparticles

The wet method was used to fabricate the silver nanoparticles (AgNPs). A magnetic stirrer was used to completely mix a 50-ml solution of 0.1M AgNO3 in deionized water after it had been made. Polyvinyl pyrrolidone (PVP) was employed to stabilize the silver nanoparticles in a second 0.1M solution (50 ml) of sodium borohydride (NaBH4). Dropwise titration was done using 50 ml of AgNO3 solution and 50 ml of NaBH4 solution. The AgNPs were separated by centrifuging the mixture at 6,000 rpm for 10 minutes while keeping it continually mixed. Prior to storage, the AgNPs underwent a 36-hour drying process in an oven set at 100°C (Siddique *et al.* 2020).

3.15.1 Nanoparticles characterization

The properties of AgNPs were confirmed using a number of instrumental techniques.

3.15.2 Spectrophotometric analysis

A UV-visible spectrophotometer was used to conduct spectral scanning (200-800 nm) in order to determine the absorption maxima of the synthesised AgNPs.

3.15.3 Scanning electron microscopy (SEM)

The scanning electron microscopy analysis revealed the dimensions and geometries of the synthesised silver nanoparticles. A cover slip grid was used to create thin films of the dried silver nanoparticle pellet. A tiny volume of solution was dropped onto the cover slip, and it was let to dry at room temperature before being seen under a scanning electron microscope. The format and distribution information about AgNPs were studied using SEM under the following conditions: Mag=2305x, signal A=SE2, HV=30.00KV, WD=12.6 mm.

3.15.4 Fourier transform infrared spectrometer (FT-IR)

The solution containing AgNPs was studied using an 8 cm-1 resolution FT-IR spectrometer (Shimadzu) in the 500-4000 cm-1 region. After mixing 1 milligramme of synthetic AgNPs with 300 milligrammes of KBr, a hydraulic pellet was formed. This pellet was further squeezed and examined using Fourier transform infrared spectroscopy. It was found that the synthesised particles exhibited functional group peaks.

3.15.5 X-ray diffraction analysis (XRD)

The size and crystallinity of the synthesised AgNPs were characterised using an XRD pattern. The sample was placed on a glass slide and the Bragg's angle θ was examined at 2° before the XRD measurements were taken. For 30 minutes, the black currant AgNPs solution was spun in a centrifuge at 10,000 rpm. We used 20 cc of deionized water to wash the pellet three times. An X'per Rota flex diffraction metre was used to compute XRD patterns from the dried AgNP combination. The parameters used were 40.0 kV voltage, 30.0 mA x-ray current, and Cu K radiation with a wavelength of 1.5406 A°. The XRD measurement was taken in 1.20 seconds using the theta-2 theta scan mode with a continuous scan speed of about 0.2000 degrees per minute and a range of 10.000 to 90.000

degrees. Using the Debye-Scherrer equation, the size of the crystallites for 35 BCSeNPs was determined (Holzwarth and Gibson 2011).

3.15.6 Calculation of MIC and MBC values

The broth macro-dilution method was used to determine the bacteriostatic and bactericidal concentration values of prepared silver nanoparticles. In sterile 10 test tubes with two control test tubes (C1: broth medium tube free of bacteria, C2: tube inoculated with the Staphylococcus bacterium only), a twofold serial concentration (2, 4, 8, 16, 32, 64, 125, 250 µg/ml) of silver nanoparticles was added in broth medium. After that, tubes containing various concentrations of AgNPs were dispensed with an 18–24-hour bacterial inoculum (5×10^6 CFU mL) and kept at 37°C overnight. The minimum inhibitory concentration (MIC) and minimum bactericidal concentrations (MBC) of drug materials were established after incubation. The lowest concentration that can result in invisible growth is MIC. Subculture has demonstrated that MBC is the lowest concentration at which bacterial growth can be stopped. For each isolate, the experiment was carried out three times, with both a negative and a positive control included (Babiker *et al.* 2020).

3.15.7 Determination of the inhibition zone

The antibacterial activity of different silver nanoparticle concentrations (100, 200, and 300 mg/mL) was tested against ten different isolates of *Staphylococcus aureus* in culture media by using the agar-well diffusion method. A nutrient broth medium was infected with a loop full of bacterial culture and left to incubate at 37°C for 24 hours. The concentration was set at 0.5 McFarland standard turbidity, which is around 108 CFU/ml. The nutrient agar plates were thinly covered with 100 µl of cell suspensions that were applied using a glass spreader. 100 microliters of each concentration of produced silver nanoparticles and 6 millilitres of dimethyl sulfoxide (DMSO) were introduced into wells with a diameter of 6 millimetres. After that, the petri dishes were placed in an aerobic

incubator set at 37°C for 24 hours. The inhibitory zones around the wells were measured to have a millimetre diameter after 24 hours. The experiments were performed three times (Rennie *et al.* 2012).

3.16 Statistical Analysis

Statistical data analysis was carried out using the popular SPSS software programme, version 32 (IBM Corp., IBM SPSS Statistics for Windows, Version 32, Armonk, NY: IBM Corp. Chicago, USA). The standard deviation and mean were used to display the quantitative data. Frequency and percentage were used to display the qualitative data. We used the analyses of variance test, the $\chi 2$-test, and the least significant difference level value, p, which was equal to or less than 0.05, in order to compare the groups (Schiefer 1980).

4. RESULTS AND DISCUSSION

4.1 Diagnosis of *Staphylococcus aureus*

The isolates of *Staphylococcus aureus* under the study were diagnosed by morphological and biochemical tests after purification on different culture media, and the results of the *Staphylococcus aureus* (*S. aureus*) colonies were translucent or opaque grey-white with a shiny surface on N/A, as shown in Figure 4.1, colonies were rounded with margins, smooth, and circular, whereas on B/A, fine with β hemolytic colonies were observed, as shown in Figure 4.2. The results of biochemical tests can be summarized in Table 4.1.

Figure 4.1 Growth of *S. aureus* on N/A

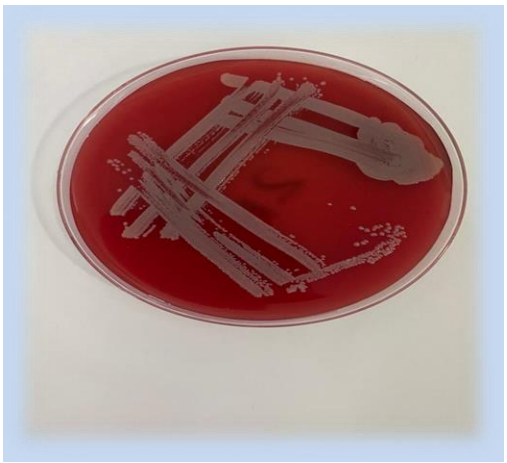

Figure 4.2 Growth of *S. aureus* on B/A

Table 4.1 The biochemical test results of *Staphylococcus aureus*

Biochemical test	Results
Oxidase	Negative
Catalase	Positive
Coagulase	Positive
Mannitol fermentation	Positive
Hemolysin	Positive
Gram stain	Positive
Urase	Positive

The API20E system

The current study showed that the results obtained using the API 20E kit are in agreement with the results obtained from phenotypic and biochemical tests for bacterial *S. aureus*.

Some characteristics of *S. aureus* should be considered to confirm the identification of this bacteria. A biochemical test by API staph identifies *S. aureus* from other staphylococci, as shown in Figure 4.3.

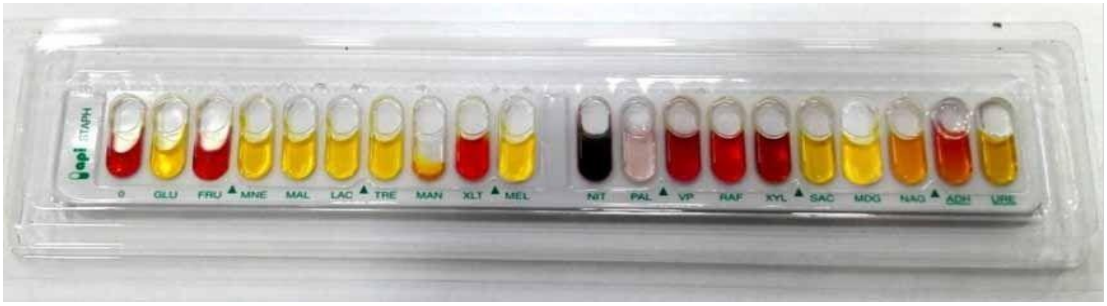

Figure 4.3 API staph system represented positive result to staph aureus, positive for GLU, MNE, MAL, LAC, TRE, NIT, MAN, MEL, NIT, PAL, VP, SAC, MDG, NAG, and ADH, while it was negative for URE, FRU, XLT, XYL, and RAF

TheVitek2 system and PCR analysis

The Vitek2 device was used for the purpose of making the final confirmation of the correctness of the diagnosis of (*S. aureus*) bacteria. This device is used to diagnose this species of bacteria after confirming (*S. aureus*) bacteria by preliminary biochemical tests. The final diagnosis results of this device for 44 bacterial isolates of (*S. aureus*) bacteria were 100%.

According to our results, the percentage of isolated (*S. aureus*) was 44 (100%) by using (PCR), as shown in Table 4.2 and Figure 4.4.

Table 4.2 Vitek2 and PCR results for the diagnosed bacterial isolates

Total examined number	Viteks		PCR (hemolysin gene)	
	Positive No.	Positive %	Positive No.	Positive %
44	44	100	44	100

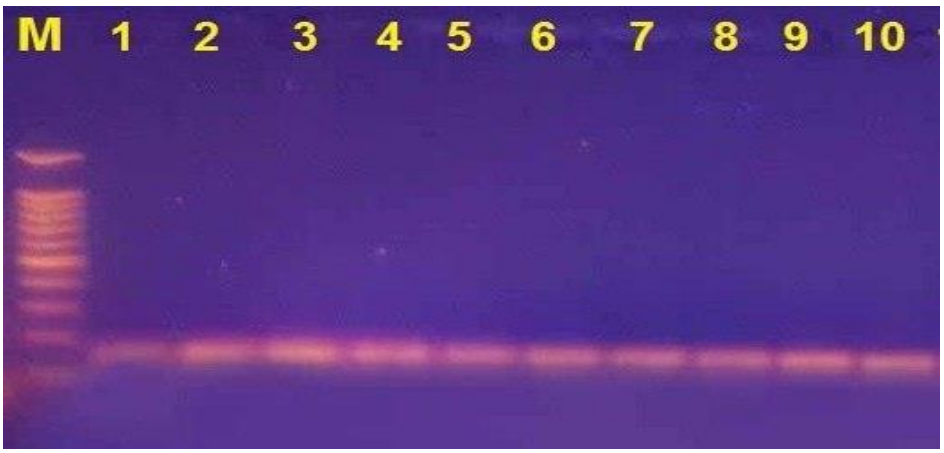

Figure 4.4 The PCR results for the α hemolysin gene in S. aureus isolates showed an expected amplification product of 186 bp. The ladder used for size comparison ranged from 100 to 1500 base pairs. The positive isolates of S. aureus were numbered 1 to 10

4.2 Clinical Bacterial Isolation

Based on our findings, the prevalence of (*S. aureus*) isolated from urine samples was 23/125 (18.4%), burn samples were 15/75 (20%), and sputum samples were 6/50 (12%), while the total sample was 44 (17.6%), as shown in Table 4.5 and Figure 4.5. At the same time, there was no marked difference (P > 0.05) in the bacterial isolation from different clinical sample types.

Table 4.5 Prevalence of *Staphylococcus aureus* isolated from different clinical samples

Type of Sample	Total Cases	Prevalence %
Urine	125	23 (18.4%)
Burn	75	15 (20%)
Sputum	50	6 (12%)
Total	250	44 (17.6%)
Calculated X^2	1.43	
Calculated P value	0.488*	

* No significant difference at P<0.05

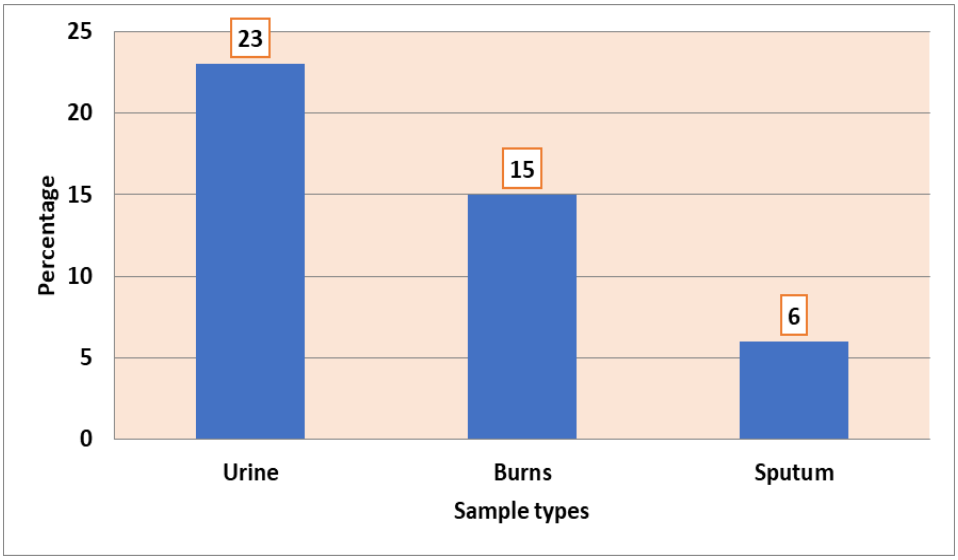

Figure 4.5 The rates of *Staphylococcus aureus* isolated from different clinical samples

4.3 Bacterial Isolation According to Gender

According to gender, the percentage of (*S. aureus*) in males was 24/110 (21.81), the percentage of (*S. aureus*) in females was 20/140 (14.28%), and the total percentage of (*S. aureus*) was 44/250 (17.6%). As shown in Table 4.6 and Figure 4.6, there was no marked difference (P > 0.05) in the bacterial distribution in males and females.

Table 4.6 Percentage of *S. aureus* according to gender

Gender	Total No.	Positive samples
Male	110	24 (21.81%)
Female	140	20(14.28%)
Total	250	44 (17.6%)
Calculated X^2	2.41	
Calculated P value	0.121*	

* No significant difference at P<0.05

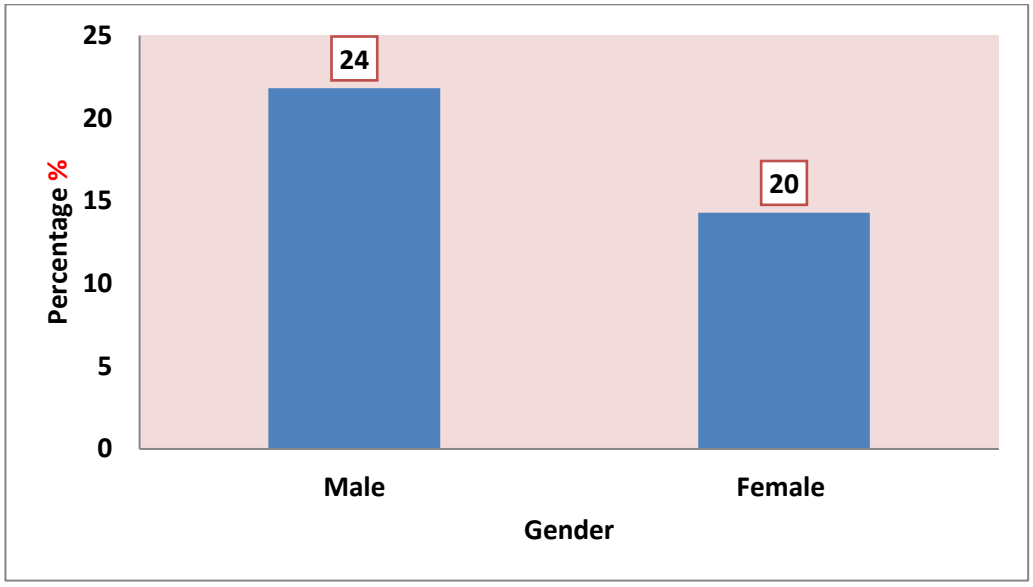

Figure 4.6 The distribution of *S. aureus* according to the gender

4.4 Bacterial Isolation According to Age

According to our results, the percentage of (*S. aureus*) was 2 (14.28%), 8 (19.51%), 14 (17.28%), 9 (21.42%), 11 (15.27%), and 44 (17.6%) among the age categories ≥ 18, 18-30, 31-40, 41-50, and 51-60, respectively. As shown in Table 4.7 and Figure 4.7, there was no statistical difference (P > 0.05) in the bacterial isolation among age intervals.

Table 4.7 Percentage of *Staphylococcus aureus* according to the age

Age group	Total No.	Positive samples
≤18	14	2 (14.28%)
18-30	41	8 (19.51%)
31-40	81	14 (17.28%)
41-50	42	9 (21.42%)
51-60	72	11 (15.27%)
Total	250	44 (17.6%)
Calculated X^2	1.01	
Calculated P value	0.908*	

* No significant difference at P<0.05

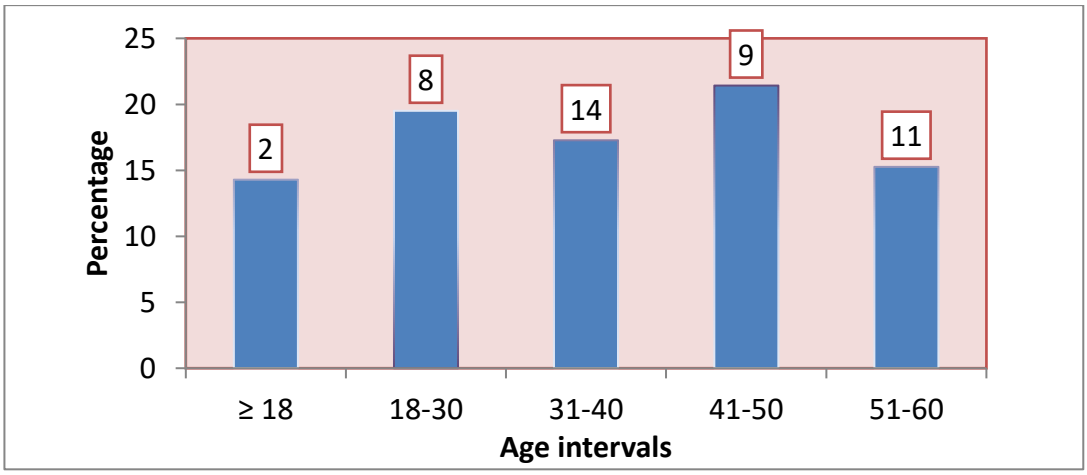

Figure 4.7 The age distribution according to *S. aureus* Positive Cases

4.5 Silver NPs Synthesis

Our study included silver NPs. Preparation was done in two steps: first, preparation of the silver nitrate solution, second, preparation of the silver NPs, as shown in Figure 4.8. Alteration of the mixture color from yellow to dark brown means that AgNPs are formed due to Ag ions reduction.

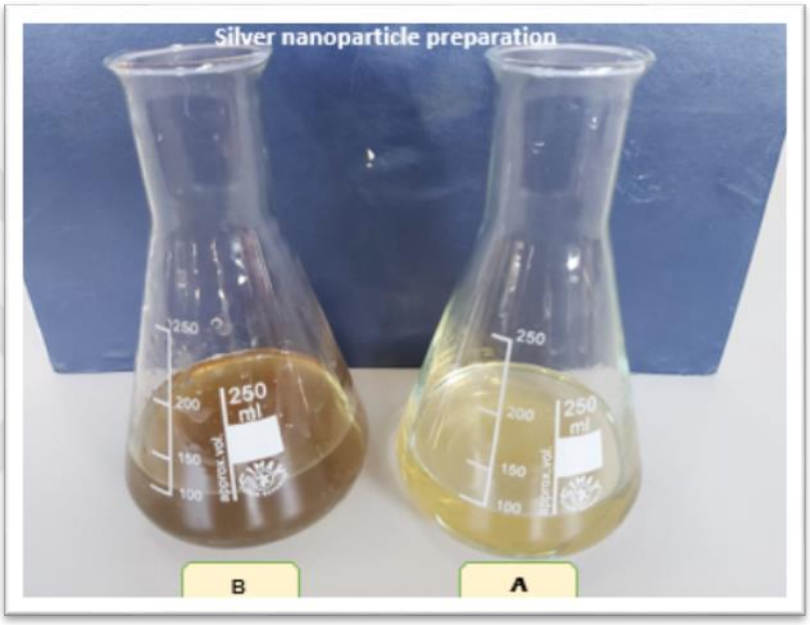

Figure 4.8 Preparation of the silver nanoparticles (A) silver nitrate solution (B) formed silver nanoparticles

4.6 Characterization of the Prepared Silver Nanoparticles

4.6.1 Uv-visible spectrophotometer

The lambda max of prepared silver nanoparticles was determined by a UV-visible range of 200–800 nm for wavelength by recording the UV-visible spectrum of the synthesized particle solution. Maximum absorbance (λ max 2.128) was shown at 418 nm, as shown in Figure 4.9.

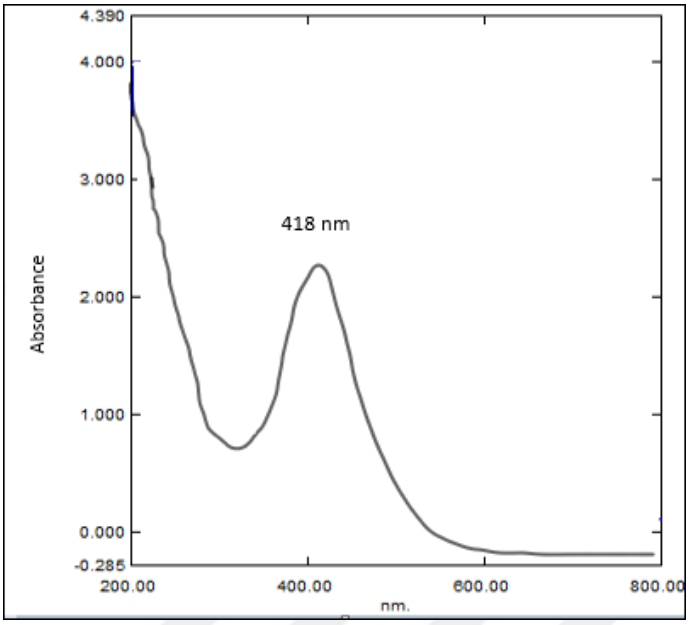

Figure 4.9 UV-visible spectrum of formed silver nanoparticle

4.6.2 The scanning electron microscopy (SEM) analysis

The scanning electron microscopy (SEM) used to determine the morphology of silver NPs regarding the crystallite size was In the SEM images included, these particles have spherical shapes and a smooth exterior. The average diameter of the obtained NPs evaluated by SEM showed a range of diameter from 38 to 98.4 nm at an average of 52.8±1.02 nm, as shown in Figure 4.10.

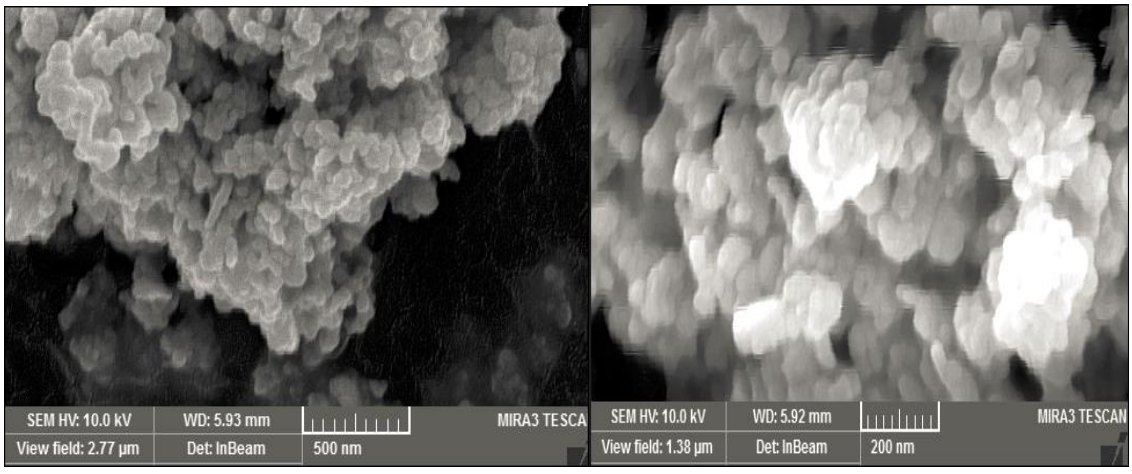

Figure 4.10 SEM of silver nanoparticles

4.6.3 The X-ray diffraction (XRD)

The X-ray diffraction (XRD) pattern in the 2Θ range of 30° to approximately 70° of the prepared AgNPs noted the presence of the various characteristic peaks, which can be indexed based on orthorhombic silver. The crystalline nature of nanoparticles was also confirmed by X-ray crystallography. The present data of XRD AgNPs recorded several main peaks at 2 Theta at 23.32, 29.69, 42.93, 43.49, 55.91, and 79.99 with their FWHM 4, 0448, 0.001, 0.556, 1.45, and 4. It was determined from the Joint Committee on Powder Diffraction Standards (JCPDS) file that the material is silver nanoparticles, as shown in Figure 4.11.

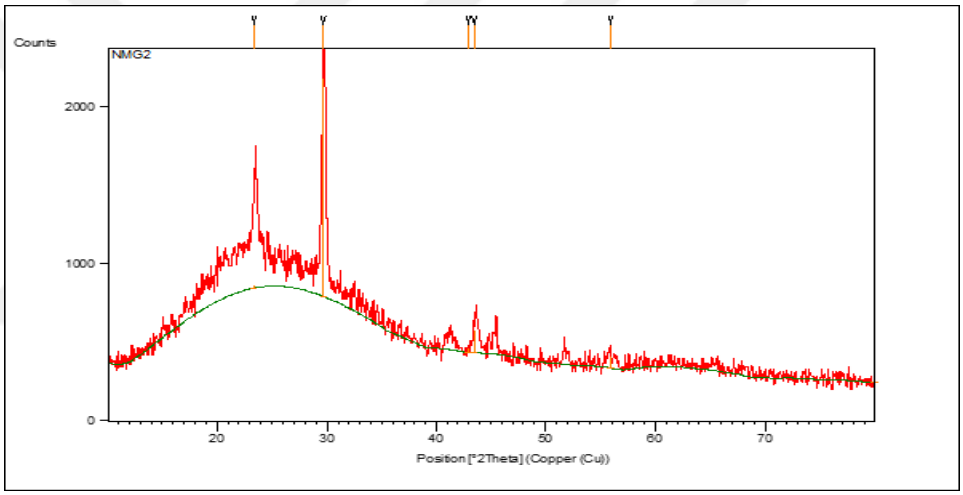

Figure 4.11 XRD of silver nanoparticles

4.6.4 FTIR analysis

The results revealed the FTIR spectrum of the freshly prepared silver nanoparticle sample. The FTIR spectrum shows absorption bands at 3441.01, 2978.09, 1786.08, 1728.2, 1577.7, 1415.7, 1365.6, 1114.86, 1014.5, and 902.6 cm^{-1}. The bands at 3441.01 cm^{-1} in the spectra correspond to the O-H stretching vibration bond. The appearance of the peak at 2978.09 cm^{-1} reveals the C-H stretching of the aromatic compound. There is another peak at 1728.2 cm^{-1} wave number linked mainly to the C-C stretching in the structure of silver nanoparticles, as shown in Figure 4.12.

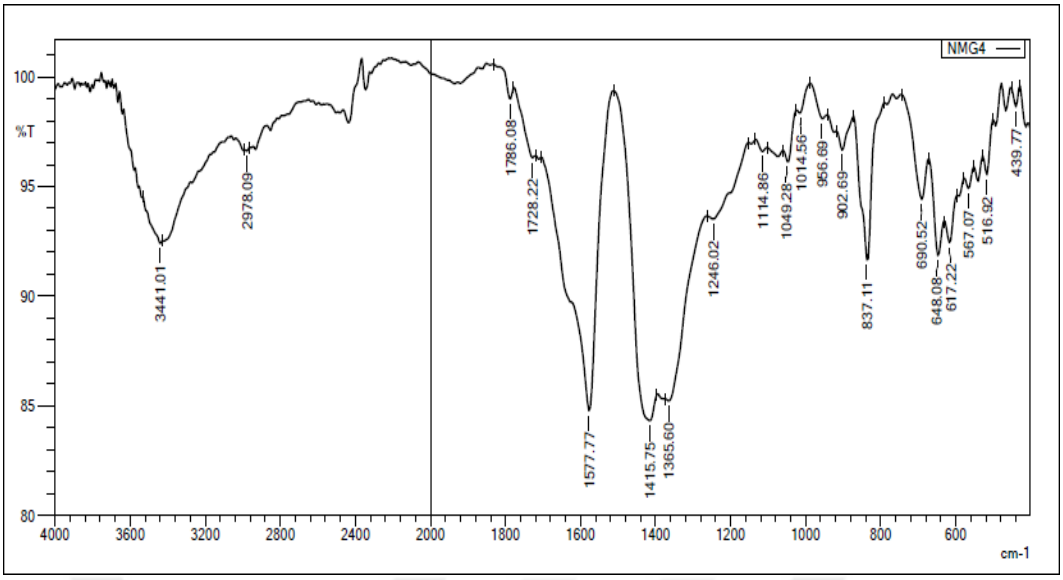

Figure 4.12 FTIR of silver nanoparticles

4.7 MIC and MBC Determination

According to Table 4.8 and Figure 4.13, the MIC values were 16, 16, 8, 32, 16, 16, 32, 32, 32, and 16 for the isolates (1 to 10), while the MBC values were 125, 125, 125, 125, 64, 125, 64, 64, 250, and 64 for the isolates (1 to 10).

Table 4.8 MIC and MBC values of prepared silver nanoparticles

No. of staph. aureus isolates	MIC value	MBC value
Isolate 1	16	125
Isolate 2	16	125
Isolate 3	8	125
Isolate 4	32	125
Isolate 5	16	64
Isolate 6	16	125
Isolate 7	32	64
Isolate 8	32	64
Isolate 9	32	250
Isolate 10	16	64
Mean± SE	**21.6±2.93**	**113.1±17.9**

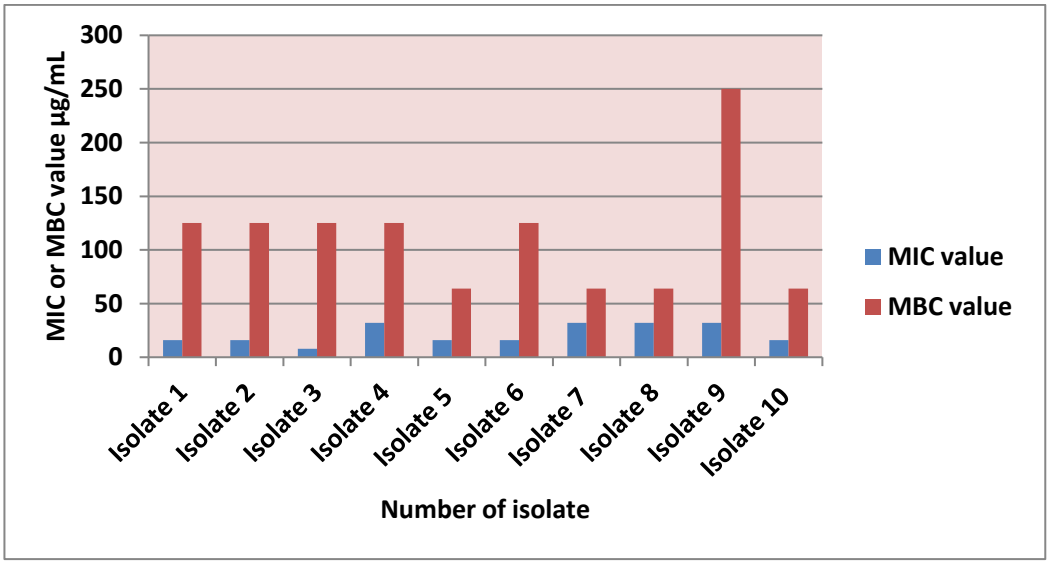

Figure 4.13 MIC and MBC values of prepared silver nanoparticles

4.8 Antibacterial Activity of AgNPs

The activity of AgNPs was examined against *S. aureus* isolates by using the agar-well diffusion method. Our findings included that the zone of inhibition of *S. aureus* (mm) (mean ± SE) was 7.47±0.16, 10.52±0.22, 14.41±0.21C, 0±0 for concentrations of silver nanoparticles (mg/mL) 100, 200, 300, and negative control (DMSO), respectively, as shown in Table 4.9 and Figures 4.14, 4.15. At the same time, the results showed that there was a proportional relationship between the concentrations of the nanoparticles and antibacterial activity.

Table 4.9 Sensitivity of isolates of *S. aureus* in culture media

The concentration of silver nanoparticles (mg/mL)	Zone of inhibition (mm) (mean ± SE)
100	7.47±0.16A
200	10.52±0.22B
300	14.41±0.21C
Negative control (DMSO)	0±0D
LSD(P<0.05)	0.652

Different letters between any two means denote to the significant difference at P<0.05

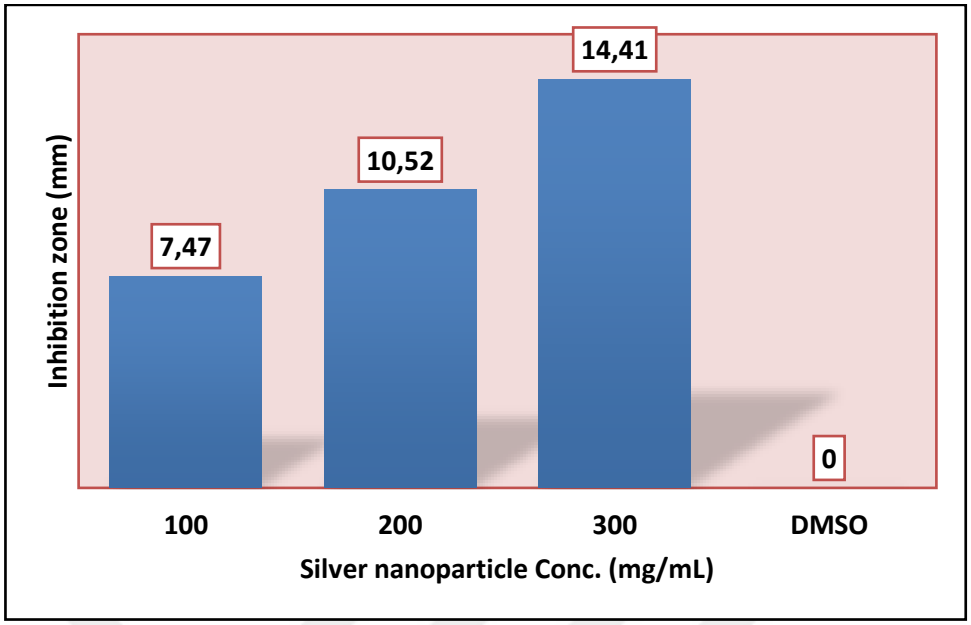

Figure 4.14 *S. aureus* sensitivity to the silver NPs concentrations

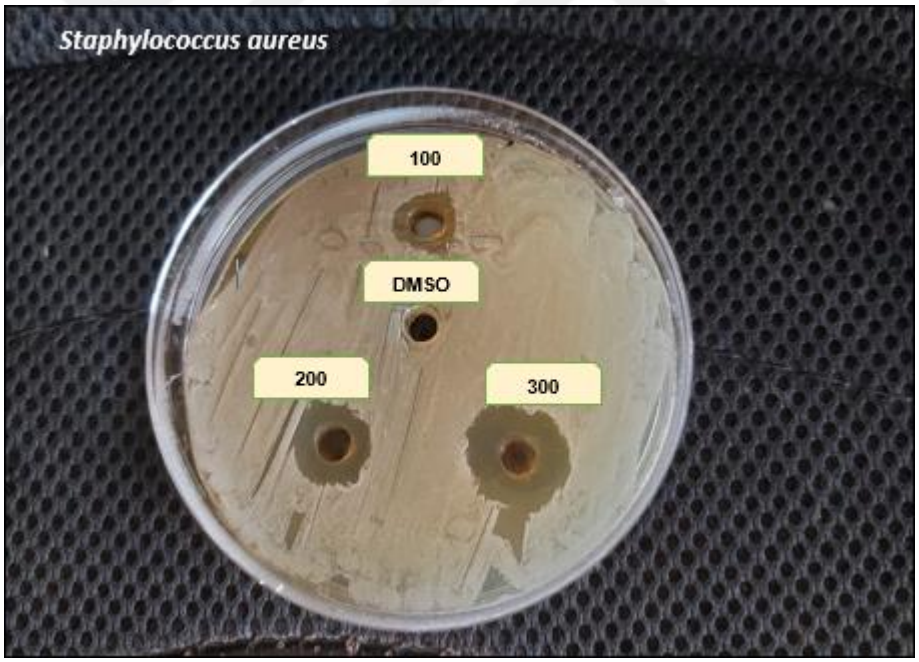

Figure 4.15 Sensitivity of the *S. aureus* to different concentrations of silver nanoparticle in culture media

4.9 Estimation the Expression of a-hemolysin Gene of *S. aureus* by Real-time PCR

Real-time PCR was used to check the expression of the a-hemolysin gene before and after the silver nanoparticles were put on *S. aureus*. The a-hemolysin gene expression (fold change) in *S. aureus* samples changed by 1 to 10 times before they were exposed to silver nanoparticles.After they were exposed to silver nanoparticles, it changed by 0.318 to 0.021 times, as shown in Table 4.10. The statistical reading revealed that there was a significant ($P<0.05$) difference in the a-hemolysin gene expression level for *S. aureus* treated with silver nanoparticles compared to the level of gene expression of the same isolate without exposure to the nanoparticles, as shown in Figures 4.10, 4.11.

Table 4.10 Molecular detection of a-hemolysin in *S. aureus* before and after exposure to the nanoparticles

The concentration of silver nanoparticles (mg/mL)	**Gene expression (fold change)**
Before exposure to silver nanoparticles	1 ± 0^{A}
After exposure to silver nanoparticles	0.318 ± 0.021^{B}
T test	8.16
P value	<0.0001

Different letters mean there are statically difference at $P<0.05$

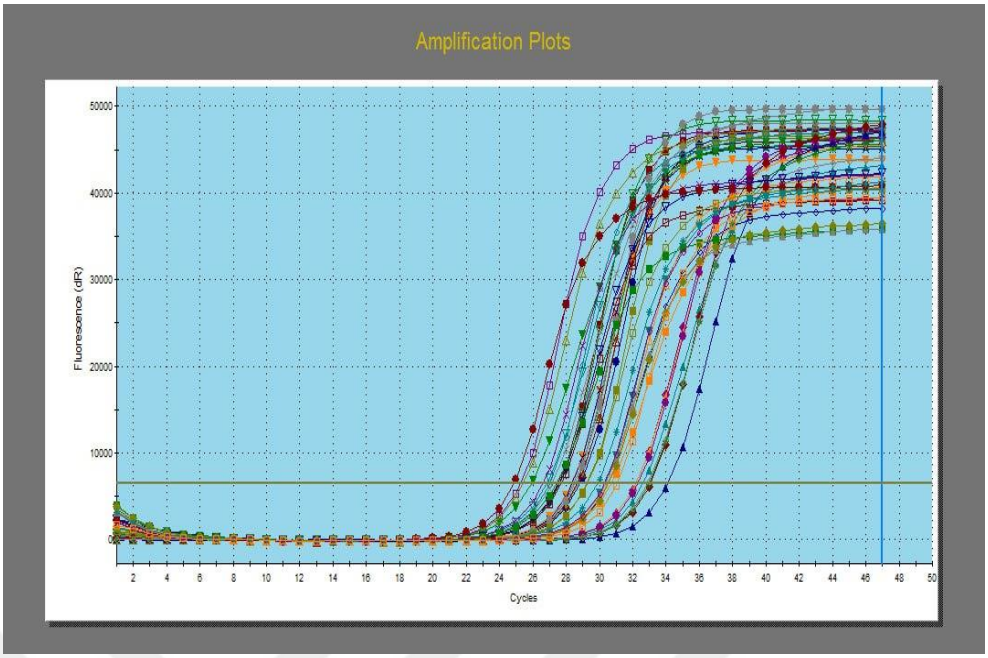

Figure 4.10 Amplification RT-PCR of a-hemolysin gene expression

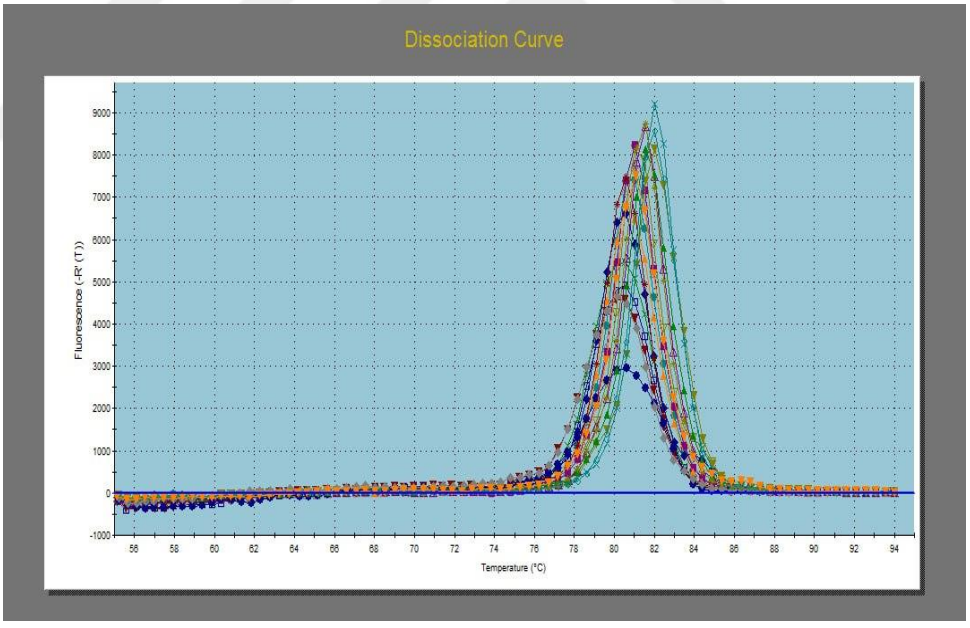

Figure 4.11 Dissociation RT PCR of a-hemolysin gene expression

4.10 Discussion

4.10.1 Diagnosis of *Staphylococcus aureus*

S. aureus was diagnosed by morphological and biochemical tests after purification on different culture media, and the study showed that (*S. aureus*) colonies were translucent or opaque gray-white with a shiny surface on N/A, colonies were circular, smooth, fine, small, and rounded with an entire margin, and all that agreement with the results of the studies of Habib *et al.* (2015), Karmakar *et al.* (2016), Taylor *et al.* (2022) found the same findings.

4.10.2 TheVitek2 system

According to our findings, Vitek2 reveals that the percentage of *S. aureus* was 100%. There are great differences in the infection rate of *Staphylococcus aureus* between the studies. One study found that the Vitek 2 system correctly identified 99.2% of 130 *S. aureus* isolates (Spanu *et al.* 2003). Another study reported that Vitek 2 identified 95% of staphylococcal isolates correctly (Nonhoff *et al.* 2005). Another study found that the Vitek 2 system correctly identified 87.5% of coagulase-negative Staphylococci isolates (Kim *et al.* 2008).

While some of the studies recorded a low rate, wherever *S. aureus* is a human pathogen, the rate was lower than 50%. 30% of the population is colonized with *S. aureus* in humans (Tong *et al.* 2015). *S. aureus* is the cause of community- and hospital-acquired bacteremia. The estimated incidence of *S. aureus* is between 20 and 30 cases per 100,000 people per year. *S. aureus* incidence ranges (38.2-45.7) for 100,000 individuals per year in the USA. *S. aureus* incidence in the industrialized world is 10–30% for 100,000 individual (Thomas *et al.* 2022).

There are several reasons for the variation in the prevalence of infection by (*S. aureus*), including genetic variation in the host and bacteria that increased susceptibility to

infection within the host and an increased capacity for virulence within the bacteria (Tong *et al.* 2015). The staphylococcal colonization rate in adults is 40%, and up to 50% of the general population is an intermittent carrier of *S. aureus* infections are more common in healthcare settings, where patients are more likely to be exposed to antibiotic-resistant strains (Messina *et al.* 2016). Staphylococcal species colonize many neonates on the skin, perineum, umbilical stump, and GI tract (Christoph and Naber, 2009). The incidence of *S. aureus* is higher in older adults. Prior exposure to antibiotics is a risk factor that is associated with high mortality in *S. aureus* infection. *S. aureus* has many virulence factors, including toxins, enzymes, and adhesins, which contribute to its pathogenicity and ability to cause infection (Thomas*et al.* 2022).

In a study in Tokyo, Japan, conducted in a tertiary care center, 52% of the patients were MRSA positive by both PCR and culture, compared to 45% who were PCR positive and culture negative (Hirokazu *et al.* 2012).

In a study consisting of 48 patients in France with culture-negative infective endocarditis, *S. aureus* was detected by PCR in 20.4% of patients (Tong *et al.* 2015). A meta-analysis of diagnostic accuracy for methicillin-resistant *S. aureus* found a significantly higher sensitivity for the overall PCR pooled estimate (92.5%) (Luteijn *et al.*2011). RT-PCR (real-time PCR) for 16S rRNA genes may be necessary in some cases to diagnose *S. aureus* infection (Taylor *et al.* 2023). Nasal PCR testing captured 81% of those colonized with MRSA (Schora*et al.* 2014).

In a study of presurgical *S. aureus* PCR assays compared with culture and post-PCR implementation surgical site infection rates, direct culture was the least sensitive for *S. aureus* (85.1%) (Tansarli *et al.* 2020). Bacterial DNA on whole blood samples could be detected in 77% of patients with positive blood cultures of *S. aureus* (Nieman *et al.* 2022).

A study published in the Journal of Clinical Microbiology found that PCR was more sensitive than culture for detecting *S. aureus* in synovial fluid samples from patients with prosthetic joint infections. The study reported a sensitivity of 91.7% for PCR compared to 66.7% for culture (Nieman *et al.* 2022). There was a systematic review and meta-

analysis of studies that looked at how well PCR could diagnose *S. aureus* bloodstream infections. The results showed that PCR had 92.3% sensitivity and 98.6% specificity (Tong *et al.* 2015). A study published in the Journal of Hospital Infection found that PCR was more sensitive than culture for detecting *S. aureus* in nasal swab samples from patients admitted to a hospital in the United Kingdom. The study reported a sensitivity of 92.5% for PCR, compared to 77.5% for culture (Schora *et al.* 2014).

A study published in the Journal of Clinical Microbiology found that PCR was more sensitive than culture for detecting *S. aureus* in bone and joint infections. The study reported a sensitivity of 91.7% for PCR, compared to 66.7% for culture. These studies suggest that PCR may be more sensitive than culture for detecting *S. aureus* infections in various clinical contexts. However, the percentage rate of *S. aureus* infections diagnosed by PCR may vary depending on the specific context and study. These percentages are specific to the particular studies mentioned and may not represent the overall percentage of *S. aureus* infections diagnosed by PCR. The use of PCR for *S. aureus* diagnosis may vary depending on the specific clinical situation, the availability of resources, health conditions, sample volume, season, environment, nature, type of sample, type of host, and general immune status (Giannoula *et al.* 2020,Tansarli *et al.* 2020).

The incidence rate of *S. aureus* in clinical symptoms might vary based on a number of different circumstances, including the particular population, the geographical area, and the time period. According to Laupland *et al.* (2013), it is advisable to check particular studies or epidemiological data for information that is more precise and up-to-date on the incidence rate of *S. aureus* in clinical symptoms.

4.11 Clinical Bacterial Isolation

Results of the current study found that the prevalence of *S. aureus* isolated from urine samples was 23/125 (18.4%), Burn samples were 15/75 (20%), andsputum samples were 6/50 (12%), while the total sample was 44 (17.6%).

The prevalence of *S. aureus* isolated from urine varies based on the population and setting being studied. A study found that *S. aureus* was 1.3% of isolates from urine specimens submitted by the community (Robert *et al.* 2006). *S. aureus* was isolated from urinary culture at (0.2–4%). *S. aureus* was common in males, long-term care, older age, urological abnormalities, and comorbidities (Mason *et al.* 2023). *S. aureus* was an infrequent urinary isolate and accounted for 1 percent of the urine (positive) (Demuth *et al.* 1979).

In addition, a different research indicated that *S. aureus* was a rare cause of UTIs in the general population, making up just 0.4–4% of urine culture positive cases (Grillo *et al.* 2020). Furthermore, according to different research designs, the prevalence of *S. aureus* bacteriuria in patients with *S. aureus* bacteremia (SAB) varies between 7.8% and 39% (Schuler *et al.* 2021).

S. aureus prevalence in burn samples is documented in many studies, wherever. In a burn treatment center in Ghana, 80 *S. aureus* isolates were obtained from 37 (60%) of the 62 patients and 13 (45%) of the 29 healthcare workers (Fritz *et al.* 2006).

In Pakistan, a study described the frequency of *S. aureus* in burn cases. The study aimed at the management of burn patients. However, the exact prevalence rate was not mentioned (Kola *et al.* 2019). Using standard culture-based techniques, the doctors at Dhaka Medical discovered MRSA. *S. aureus* was identified in 44.44 percent of burn wound samples, with 22.25 percent of those isolates displaying resistance to oxacillin (Islam *et al.* 2013). In a hospital in Morocco, the predominant bacteria isolated were *S. aureus* (33.85%) (Humphries *et al.* 2022). In the Yekatit 12 Hospital Burn Unit, Addis Ababa, Ethiopia, *S. aureus* was one of the pathogens in the burn. However, the exact prevalence rate was not mentioned (CDC 2019).

S. aureus is isolated from burn cases, so the high rate of MDR *S. aureus* was occurring in the burn centers. In burn cases, *S. aureus* can produce the biofilms (Al-Talib 2016).

In a study conducted in Albania, the prevalence of *S. aureus* in hospitalized cases was 34.2%, but the study did not specifically focus on sputum samples (Kika *et al.* 2020). In a study conducted in USA, the prevalence of *S. aureus* nasal colonization was 1.5% (Matthew *et al.* 2006).

S. aureus prevalence in septum in *S. aureus* bacteremia cases ranged between 7.8% and 39%, depending on the study design. Prevalence rates may vary depending on factors such as the population studied, the presence of risk factors, and the specific healthcare setting (Schuler *et al.* 2012).

The prevalence of *Staphylococcus* infection can differ according to the type of sample taken due to various factors. The prevalence of *Staphylococcus* infection in a specific sample type may depend on the natural colonization patterns of the bacteria at that particular site (Matthew *et al.* 2006). The prevalence of *Staphylococcus* infection can be influenced by exposure to the bacteria, and the mode of transmission, such as UTIs, may be influenced by contaminated catheters. Burn infections may be more common in people with poor health conditions (Tong *et al.* 2015). *Staphylococcus* infection rates can vary depending on host age and immune status. The rate of *S. aureus* in adults is higher in elderly individuals with compromised immune systems as compared with healthy individuals. The rate of *staphylococcus* is influenced by the sensitivity and specificity of the used techniques and sample source (Kates *et al.* 2018).

4.12 Bacterial Isolation According to Gender

According to our findings, the percentage of *S. aureus* in males was 24/110 (21.81), the percentage of *S. aureus* in females was 20/140 (14.28%), and the total percentage of *S. aureus* was 44/250 (17.6).

In a study, it was found that *S. aureus* occurs mostly in males and more in females (Tong *et al* 2015). The prevalence of *S. aureus* was 41.0% in male patients and 44.2% in female patients (Smit *et al.* 2017). The prevalence of *S. aureus* in fitness facilities was 26.7% in

males and 11.5% in females (Dalman *et al.* 2019). In nasal infection, *S. aureus* prevalence in males was 32.4%, while in females it was 30.7% (Matthew *et al.* 2006). The ratio rate of male-to-female MSSA BSI was 1.63, while MRSA BSI was 1.72 (Hilary *et al.* 2015). The *S. aureus* incidence of skin infection was greater in the males than in the females (Castleman *et al.* 2018).

S. aureus percentage in males and females may vary based on the type of the studied population, the exposure rate for bacteria, and the colonized tissue type. The males have a higher percentage of the nasal infection with *S. aureus* than the females (Castleman *et al.* 2018).

Another study found that males may be more likely to be exposed to *S. aureus* in certain settings, such as fitness facilities, which can increase their risk of infection (Van Hal *et al.* 2012). The males may be more attractive to the sepsis than the females. Another study found that the prevalence of hand hygiene is different based on gender, females may be more likely to practice good hand hygiene than males, which can reduce their risk of infection. Males may have a higher carriage rate of *S. aureus* than females on the hand and external layers of the skin, which can increase their risk of infection (Humphreys *et al.* 2015).

4.13 Bacterial Isolation According to Age:

The results showed that the percentage of *S. aureus* was 14.28%, 19.51%, 17.28%, 21.42%, 15.27%, and 17.6% among the age categories ≥ 18, 18-30, 31-40, 41-50, and 51-60, respectively. Our results found that a higher rate occurred in categories 31–40 years, while a lower rate occurred in category ≥ 18 years.

In a study conducted in Denmark, the incidence of *S. aureus* bacteremia increased with age, with the largest change in incidence observed for persons over 80 years old (Thorlacius *et al.* 2019). Age has a role in *S. aureus* incidence, there is a high prevalence at the life extreme (Tong *et al.* 2015). In Minnesota, the median age of *S. aureus* infection

was 57 years, with a range of 1–97 years. In hospital-onset cases, the median age was 57 years, in community-onset cases and healthcare-associated cases, it was 63 years, and in community-associated cases, it was 46 years (Minnesota Department of Health, 2022). In Auckland, New Zealand, the median age of patients with *S. aureus* was 22 years (Williamson *et al.* 2013). According to Tong *et al.* (2015), the incidence of *S. aureus* varies based on age, with the highest rate occurring in individuals who are more than 65 years old.

According to research published in 2019 by Thorlacius *et al.*, age-related changes in the immune system may cause older people to have a weakened immune system. As a consequence, older adults are more likely to get infected with *S. aureus*. There is a connection between comorbidities associated with aging and an increased risk of contracting a *S. aureus* infection. Some of these comorbidities include respiratory disorders, diabetes, and heart problems. This kind of comorbidity tends to be more common in people of advanced age, which helps explain why infections are more common in people of this age range. It is probable that older people will have more frequent encounters with the medical system, such as stays in hospitals and other long-term care facilities, as well as invasive procedures.

According to Kang *et al.*'s (2011) research, exposure to specific aspects of the healthcare industry may increase one's risk of contracting a *S. aureus* related illness. It is possible for *S. aureus* to colonize the skin, and how much this occurs depends heavily on the person's age. Williamson *et al.* (2013) state that the higher colonization rates that are shown in older individuals and infants may be the reason for the higher infection rates that is shown in both age groups. Additionally, they state that the higher colonization rates that are seen in newborns may also be the cause of the higher infection rates. Differences in hygiene practices and exposure patterns can also contribute to the variation in *S. aureus* incidence among different age groups. The younger individuals may have higher rates of community-associated infections due to factors such as close contact in schools or sports activities (Van *et al.* 2012).

4.14 Silver NPs Synthesis

Our study included silver NPs. Preparation was done in two steps: first, preparation of the Ag nitrate, and second, preparation of the silver NPs. The reaction mixture color changed from yellow to dark brown (AgNPs formation) due to the reduction of Ag ions to Ag nanoparticles.

A study found that the phytosynthesis process of silver nanoparticles is done by using plant extract. The optimum synthesis of Ag NPS has spent 60 seconds at pH 8 and AgNO 3 concentrations of 1 mM and 70°C. Ag NPS produced under these circumstances is crystalline, primarily spherical, with some rod- and triangle-shaped particles also present, with diameters of 37–44 nm. The functional groups of the stem extract's phenolic, carboxyl, and amine chemicals are what help reduce Ag ions(Vanaja *et al.* 2013).

In another study, the synthesis of AgNPs was done by using Silybum marianum fruit extract. The separation of NPS was done by using the centrifuge. Reduction of the silver after exposure to S. marianum extract causes a color change from colorless to dark within one day. AgNP particle size showed 2θ around 25 nm. Synthesized Ag NPS by silymarin seems to be spherical in shape (Ayad *et al.* 2019).

Hagenia abyssinica was used for the bio-reduction of silver nitrate in order to synthesise AgNPs. AgNP formation was confirmed. Synthesized AgNPs showed maximum absorption at 430 nm. The synthesized AgNPs showed antimicrobial and antioxidant activities (Melkamu and Bitew 2021).

AgNPs are prepared based on Ag nitrate and starch. The color is changed from colorless to dark through the Ag nitrate. The starch reduces Ag ions into Ag NPS within one hour. AgNPs have antibacterial effects against *S. aureus, S. pyogenes, S. typhi,* and *P. aeruginosa*. The zone diameter increases with increasing AgNP concentration. Higher inhibition of *S. aureus* (16.4 mm), then *P. aeruginosa, S. pyogenes*, and *S. typhi* (10.4 mm) was observed (Yakout and Mostafa 2015).

Aniline and silver nitrate are used as the reductant and oxidant, respectively, to characterize AgNPs. At 400 nm, a large SRP band appears, demonstrating the spherical nature of the AgNPs. AgNPs formed stunning silver nanocrystals as a result of their asymmetrical aggregation. Through electrostatic, van der Walls, and hydrogen bonding interactions, aniline adsorbed onto the surface of Ag NPS (Zaheer *et al.* 2017).

The product metabolites of actinomycetes strains *Streptomyces rochei* and *Microbacterium proteolyticum* are used to synthesize AgNPs at 37 °C for 7 days. AgNPs have antibiofilm and antibacterial effects against meningitis-causing bacteria. AgNPs revealed peaks with positions of 1637.17 cm1 and 1636.10 cm1 for the C=O amide group. These NPs were effective against *S. pneumoniae, N. meningitides*, and *H. influenza* (Bano *et al.* 2023).

Using Saraca asoca aqueous leaf extract, the synthesis of AgNPs was performed. AgNPs that had been synthesized had been evaluated before being stored in the best possible way. Throughout the 18-month testing period, AgNPs showed great stability and outstanding dispersity. Both of the tested strains were successfully inhibited by AgNPs' adequate antibacterial activity. The particles that had been stored for two to six months showed the greatest rate of inhibition. The antibacterial properties of the particles start to fade after six months (Habibullah *et al.* 2022).

Through the production of starch and Ag NPS, AgNPs were created. The alkali in the starch acts as a stabilizing agent for the produced AgNPs as well as a reducing agent for Ag ions. The chemical reduction procedure took place in a water bath while being homogenized quickly. Using ethanol as a precipitant, AgNPs coated with starch were cooled. Centrifugation was used to separate the powder precipitate, which was then cleaned and dried. Pure AgNPs are typically less than 20 nm in size, spherical in form, and have a high level of AgNPs (30000 ppm). AgNPs coated with starch have greater heat stability than starch nanoparticles alone. According to the results of the analyzer for particle size and zeta potential analysis, St-AgNPs have excellent homogeneity and great stability (Hebeish *et al.* 2013).

In a different study, it was discovered that soil microorganisms were examined for their capacity to produce AgNPs. The isolated soil bacteria are capable of biosynthesising AgNPs. Optimizations were used to examine five independent variables. The biosynthesis of AgNPs has a 423 nm absorption peak, a spherical shape, and a mean particle size of 17.43 nm. All of these properties were visible. The bands at 3321.50, 2160.15, and 1636.33 cm1 represent the alkyne nitrile, amine, and amine bands, respectively. AgNPs have demonstrated antibacterial efficacy against a number of significant diseases in medicine. With the exception of *K. pneumoniae*, which has a greater MIC of 1000 g/mL, all microbiological pathogens had MIC values for AgNPs of 500 g/mL (Abdelmoneim *et al.* 2022).

4.15 Characterization of the Prepared Silver Nanoparticles

4.15.1 Uv-visible spectrophotometer

The lambda max of prepared silver nanoparticles was determined by a UV-visible spectrophotometer at 200–800 nm for wavelength by recording the UV-visible spectrum of the synthesized particle solution. Maximum absorbance (λ max 2.128) was shown at 418 nm.

To determine how much light is absorbed or transmitted in the visible and ultraviolet (UV and VIS) parts of the electromagnetic spectrum, one may use a UV-visible spectrophotometer (Agustina *et al.* 2021, Ashraf *et al.* 2016). The maximum wavelength at which a substance's absorption spectra show the highest intensity, or lambda max, is denoted as λmax. A UV-visible spectrophotometer can detect this trait, which is unique to the chemical (Agustina *et al.* 2021).

Ag NPS are small particles with sizes ranging from 1 to 100 nanometers. They have unique optical, electrical, and antimicrobial properties, making them useful in various applications, such as electronics, catalysis, and medicine. The absorption spectrum of

silver nanoparticles typically exhibits a maximum absorption peak in the UV-visible range due to a phenomenon called surface plasmon resonance (Gondwal *et al.* 2018).

The range of 200–800 nm refers to the wavelength range in the UV-visible spectrum that can be measured using a UV-visible spectrophotometer. This range covers both the UV and visible regions of the electromagnetic spectrum (Agustina *et al.* 2021, Jose *et al.* 2022). The given information suggests that the higher absorption of Ag NPS occurred at a wavelength of 418 nm. This indicates the λmax for the absorption spectrum of the Ag NPS (Ashraf *et al.* 2016, Fu *et al.* 2021). And that showed agreement with our results.

4.15.2 SEM analysis

(SEM) used to determine the morphology of silver NPs regarding the crystallite size was In the SEM images included, these particles have spherical shapes and a smooth exterior. The average diameter of the obtained NPs evaluated by SEM showed a range of diameter from 38 to 98.4 nm at an average of 52.8±1.02 nm.

(SEM) is used to take images of the sample surface with a focused beam of electrons (Sampathkumar *et al.* 2020). It is commonly used in the characterization of Ag NPS to study its size, shape, and morphology (Puchalski *et al.* 2007, Goudarzi *et al.* 2016, Khan*et al.* 2019).

Silver nanoparticle size, shape, and distribution may all be seen visually in SEM pictures. According to studies by Yi *et al.* (2013), Goudarzi *et al.* (2016), and Tzu-Lan *et al.* (2018), these pictures may reveal the location of individual nanoparticles inside a sample. To examine the ingredients, NPS, EDX, and SEM are often combined. Data regarding the chemical elements is provided by EDX (Puchalski *et al.* 2007, Goudarzi *et al.* 2016).

The sample surface's topographical investigation using SEM may also provide details regarding the surface's texture, roughness, and surface characteristics (Sampathkumar *et al.* 2020). Silver nanoparticles' crystalline structure may be examined using SEM. In order

to achieve this, it is possible to look at the diffraction patterns that the nanoparticles create (Goudarzi *et al.* 2016, Khan *et al.* 2019).

SEM is used for characterizing silver nanoparticles. It allows researchers to visualize the size, shape, and distribution of the nanoparticles, analyze their elemental composition, and study their crystallographic structure. The mentioned studies found data that supports our results.

4.15.3 XRD analysis

The current study showed that the XRD pattern in the 2Θ range of 30° to approximately 70° of the prepared AgNPs noted the presence of the various characteristic peaks, which can be indexed based on orthorhombic silver. X-ray crystallography also confirmed the crystalline nature of nanoparticles. The present data on XRD AgNPs recorded several main peaks, which were 2 Theta at 23.32, 29.69, 42.93, 43.49, 55.91, and 79.99 with their FWHM 4, 0448, 0.001, 0.556, 1.45, and 4. It was determined from the JCPDS file that the material is silver nanoparticles.

The crystal structure and size of materials, including silver nanoparticles, are determined via XRD analysis. By using XRD analysis, it is possible to confirm the existence of silver nanoparticles and their crystal structure. According to the silver crystal planes, the XRD shows distinctive peaks (Theivasanthi and Alagar 2011, Gurunathan *et al.* 2015, Koohpeima *et al.* 2017).

XRD analysis reveals the structure of silver nanoparticles. The existence of a face-centered cubic (FCC) crystal structure may be inferred from the peaks in the XRD pattern that can be indexed to certain crystal planes, such as (111), (200), and (220) (Gurunathan *et al.* 2015, Koohpeima *et al.* 2017).

The mean crystalline size of Ag NPS may be determined via XRD examination. The Debye-Scherrer formula, which considers the instrumental broadening of the peaks, may

be used to calculate crystal size (Koohpeima *et al.* 2017). The Scherrer equation, which connects the width of the observed diffraction line at its half-intensity maximum, the wavelength of the X-ray source, and a shape factor, may be used to determine the crystallite diameter (Dc) of silver nanoparticles (Gurunathan *et al.* 2015).

The experimental outcomes and theoretical values may also be compared using XRD analysis. The unit cell edge of the FCC crystal structure is compared with the traditional value, as well as the computed crystalline size with the size estimated using other methodologies (Koohpeima *et al.* 2017).

Based on the JCPDS file, it was established that the substance was silver nanoparticles. The peaks in the XRD pattern were linked to the (111), (200), and (220) planes of silver. These planes fit with the face-centered cubic (FCC) structure of silver (Mehta *et al.* 2017). The XRD test also showed the average crystalline size of the silver nanoparticles. This size can be guessed using the Debye-Scherrer formula and the Scherrer equation. The resultant particles are Ag NPS with an FCC structure obtained by XRD, which provides data about the crystalline size. It allows for the comparison of experimental results with theoretical values and helps in understanding the structural properties of silver nanoparticles (Bykkam *et al.* 2015).

4.15.4 FTIR analysis

Our findings showed that the FTIR spectrum of the freshly prepared silver nanoparticles sample shows absorption bands at 3441.01, 2978.09, 1786.08, 1728.2, 1577.7, 1415.7, 1365.6, 1114.86, 1014.5, and 902.6 cm^{-1}. The stretching vibration link between oxygen and hydrogen is represented by the bands at 3441.01 cm^{-1} in the spectra. The aromatic compound's C-H stretching is seen by the peak at 2978.09 cm^{-1}. The major association between the 1728.2 cm^{-1} wave number and the C-C stretching in the silver nanoparticle structure is another peak. FTIR is used to analyze the functional groups in Ag-ion AgNPs (Tag *et al.* 2021).

FTIR analysis can help identify the functional groups involved in the reduction of silver ions to AgNPs (Tag *et al.* 2021). Other techniques used to characterize silver nanoparticles include UV-visible spectroscopy (UV-vis), X-ray diffraction (XRD), dynamic light scattering (DLS), and transmission electron microscopy (TEM) (Gurunathan *et al.* 2018).

These techniques determine the shape, size, and crystallographic plane of the NPS, as well as their stability and surface charge (Tag *et al.* 2021) (Gurunathan *et al.* 2018). In addition, cytotoxicity assays can be used to evaluate the potential toxicity of silver nanoparticles (Gurunathan *et al.* 2018, Nasar *et al.* 2019, Naveed *et al.* 2022, Rudrappa*et al.* 2022).

4.16 MIC and MBC Determination

For the *S. aureus* isolates (1–10), the MIC values were 16, 16, 8, 32, 16, 16, 32, 32, 32, and 16. The MBC values were 125, 125, 125, 125, 64, 125, 64, 64, 250, and 64 for the isolates (1–10).

A study found that the MIC value of silver nanoparticles on *S. aureus* isolates was 0.015 mg/mL (Sedrizadeh-Bami *et a.l.* 2020). In another study, it was found that the MIC value for silver nanoparticles against *S. aureus* ATCC 29213: 0.062 µg/mL against some food pathogens (Hatipoğlu 2022).

MIC values depend on the strain of *S. aureus,* the level of silver nanoparticles, and the experimental conditions.

4.17 Antibacterial Activity of AgNPs

The activity of AgNPs was examined against *S. aureus* isolates by using the agar-well diffusion method. Our findings included that the zone of inhibition of *S. aureus* (mm) was 7.47, 10.52, 14.41, and 0±0 for levels of silver nanoparticles (mg/mL) 100, 200, 300, and negative control (DMSO), respectively. At the same time, there was a proportional

relationship between the NPS levels and the antibacterial effects. The present results found that as the used dose was larger, the inhibition zone was greater.

A study found that AgNPs (4) μg/ml prevents the growth of *S. aureus* (Fateme *et al.* 2011, Attallah *et al.* 2022). AgNPs exhibited antibacterial activity against *S. aureus* that was isolated from different clinical conditions, as they resulted in clear zones around the AgNPs discs by disc diffusion assay (Mirzajani *et al.* 2011). Cell wall damage is produced by AgNPs as well as the accumulation of AgNPs in the bacterial membrane. Increasing AgNP to 8 μg/ml leads to the production of muramic acid, which is attributed to cell wall distraction (Dakal *et al.* 2016), and that agrees with our findings. AgNPs have antibacterial activity against *S. aureus*, which reveals that the growth of *S. aureus* is done due to the fact that Ag ions interact with DNA, leading to the prevention of cell reproduction and division (Dakal *et al.* 2016). AgNPs have antibacterial activity effects on *E. coli* and *S. aureus* (Xing *et al.* 2021). In addition to that, Ag-NPs have a wide range of antimicrobial effects that kill and inhibit gram-positive and negative pathogens, all of which support our results (Li *et al.* 2011).

In a study comparing the inhibition zones of AgNPs against *S. aureus*, the average zone of inhibition for *S. aureus* was reported to be 7.0 mm (Vu *et al.* 2018).

The study also compared the inhibition zones of silver ions to those of AgNPs. The areas where silver ions and AgNPs stopped the growth of *E. coli* were similar, but the areas where *S. aureus* grew faster were bigger (Vu *et al.* 2018). Another study demonstrated that AgNPs (4) μg/ml inhibited *S. aureus* growth (Fateme *et al.* 2011). The MIC of AgNPs on *S. aureus* was 2 μg/mL (Thammawithan *et al.* 2021).

The observed inhibition zones on agar plates are evidence that AgNPs have an inhibitory effect on the growth of *S. aureus*-, according to these findings. The size of the inhibition zone can vary depending on factors such as the concentration of used AgNPs, the specific experimental conditions, and the type of pathogens (Yuan *et al.* 2017).

4.18 The Gene Expression of α-hemolysin Gene in *S. aureus*

Based on the current results, the gene expression of the a-hemolysin gene in isolates of *S. aureus* that were exposed to silver NPS was lower (0.318) than in the control group.

It was discovered in research that investigated the impact of ZnO NPS influence on the production of the hemolysin gene in *S. aureus* that the expression of the gene was greatly decreased (Saghalli *et al.* 2016, Liao *et al.* 2017). This was shown to be the case in both of the studies. Another study assessed the antibacterial efficiency of Ag NPs against *S. aureus* and found that SNPs suppressed the well-known virulence component hemolysin (Soleimani and Habibi-Pirkoohi 2017). This finding was based on the observation that SNPs decreased the activity of the bacterium. Research was conducted in which nanocurcumin-capped AuZnO nanocomposites were used to explore the reduction of hemolysin in *S. aureus*. According to *Jabir et al.* (2022), the findings demonstrated that the nanoparticles acted as an antibacterial agent and were able to kill bacterial cells by causing a reduction in the synthesis of hemolysin. According to research carried out by Kong *et al.* (2016), silver nanoparticles have the potential to prevent *S. aureus* from producing beta-hemolysin and from forming biofilms.

Research was conducted to determine whether the expression level of the virulence genes in *S. aureus* was affected by silver nanoparticles, also known as AgNPs. According to the findings, AgNPs dramatically suppressed the expression of a number of virulence genes, including the hemolysin gene (Hamida *et al.* 2020). In a separate piece of research, the influence that AgNPs have on the expression of the virulence genes in MRSA strains was investigated. AgNPs dramatically downregulated the expression of the hemolysin gene and other virulence genes, suggesting that AgNPs may be a viable treatment agent for MRSA infections (Yan *et al.*, 2022). These findings were published in the journal Yan *et al.* (2022). Research was conducted to evaluate the impact that ZnO NPs have on the expression of virulence genes in *S. aureus*. According to Abdelghafar *et al.* (2022), the fact that ZnO NPs were able to reduce the expression of the hemolysin gene as well as other virulence genes suggests that ZnO NPs have the potential to be used as a therapeutic treatment for *S. aureus* infections.

An investigation of the impact of AuNPs on the expression of virulence genes in *S. aureus* has been carried out. The findings demonstrated that AuNPs decrease the expression of the hemolysin gene as well as other virulence genes, suggesting that AuNPs may be a viable therapeutic agent for *S. aureus* infections (Villa-Garcia *et al.* 2021). And these findings were published in the journal (Villa-Garcia *et al.* 2021).

These findings provide evidence that several kinds of nanoparticles, such as AgNPs, ZnO NPs, and AuNPs, have the potential to inhibit the expression of the hemolysin gene in *S. aureus*. According to Arunachalam *et al.* (2023), in order to get a complete understanding of the mechanism of action of nanoparticles on the expression of hemolysin and their prospective application as antibacterial agents, more study is required.

According to these results, Ag NPS suppresses the production of the hemolysin gene in *S. aureus*, which is a key virulence factor that may or may not be caused by processes that are known or understood. The findings of the research that were cited before corroborate our findings.

5. CONCLUSIONS AND RECOMMENDATIONS

Conclusions

1. *Staphylococcus aureus* is a major pathogen capable of causing diverse infections due to an array of virulence factors and its ability to form biofilms.
2. The pore-forming toxin α-hemolysin is an important part of *S. aureus*'s pathogenicity because it damages host cell membranes.
3. AgNPs exhibit broad-spectrum antibacterial activity against *Staphylococcus aureus* and other pathogens through multiple mechanisms, including cell membrane damage.
4. AgNPs can inhibit *S. aureus* growth and suppress the production of virulence factors like α-hemolysin.

Recommendations

1. Further research is needed to better understand the complex regulatory networks controlling virulence gene expression in *S. aureus* during different stages of infection. Virulence determinant production is affected by things like bacterial density, stress responses, host signals, and regulatory circuits. Figuring out how these things work could lead to new therapeutic targets.
2. The combination of AgNPs with antibiotics or other therapeutic agents may provide synergistic benefits against *S. aureus*.
3. Silver nanoparticles represent a promising antibacterial approach but require extensive cytotoxicity testing before therapeutic applications.
4. Evaluate combinations of AgNPs with other nanoparticles like zinc oxide for enhanced activity against *S. aureus*.
5. Develop green synthesis methods for AgNPs using plant extracts and assess their antibacterial effects.

REFERENCES

Ajitha, B., Reddy, Y. A. K. and Reddy P. S. 2014. Biosynthesis of silver nanoparticles using Plectranthus amboinicus leaf extract and its antimicrobial activity. Spectrochimica Acta Part A: Molecular and Biomolecular Spectroscopy, 128: 257-262.

Akhtar, M. S., Panwar, J., Yun, Y. S. 2013. Biogenic synthesis of metallic nanoparticles by plant extracts. ACS Sustain. Chem. Eng., 1: 591–602.

Aljanaby, A. A. J., and Alhasani, A. H. A. 2016. Virulence factors and antibiotic susceptibility patterns of multidrug resistance Klebsiella pneumoniae isolated from different clinical infections. African Journal of Microbiology Research, 10(22), 829-843.

Alshareef, A., Laird, K., Cross, R. B. M. 2017. Shape-dependent antibacterial activity of silver nanoparticles on Escherichia coli and Enterococcus faecium bacterium. Appl. Surf. Sci., 424: 310–315.

Al-Thabaiti, S. A., Aazam, E. S., Khan, Z., Bashir, O. 2016.Aggregation of Congo red with surfactants and Ag-nanoparticles in an aqueous solution.Spectrochim. Acta Part A Mol. Biomol. Spectrosc, 156: 28–35.

Anjum, S., Abbasi, B. H. and Shinwari, Z. K. 2016. Plant-Mediated Green Synthesis of Silver Nanoparticles For Biomedical Applications: Challenges And Opportunities. Pakistan Journal of Botany, 48(4): 1731-1760.

Arvidson, S., Tegmark, K. 2001. Regulation of virulence determinants in *Staphylococcus aureus* . International Journal of Medical Microbiology, 291(2): 159–170.

Balaji, D. S., Basavaraja, S., Deshpande, R., Mahesh, D. B., Prabhakar, B. K., Venkataraman, A. 2009. Extracellular biosynthesis of functionalized silver nanoparticles by strains of Cladosporium cladosporioides fungus. Colloids Surf. B Biointerfaces, 68: 88–92.

Banerjee, P., Satapathy, M., Mukhopahayay, A., Das, P. 2014. Leaf extract mediated green synthesis of silver nanoparticles from widely available Indian plants: Synthesis, characterization, antimicrobial property and toxicity analysis. Bioresour. Bioprocess, 1: 3.

Bantel, H., Sinha, B., Domschke, W., Peters, G., Schulze-Osthoff, K., Jänicke, R. U. 2001. α-toxin is a mediator of *Staphylococcus aureus*-induced cell death and activates caspases via the intrinsic death pathway independently of death receptor signaling. Journal of Cell Biology, 155(3): 637–647.

Bapat, R. A., Chaubal, T. V., Joshi, C. P., 2018. An overview of application of silver nanoparticles for biomaterials in dentistry. Mater Sci Eng C., 91: 881–898.

Barakat, K. M., El-Sayed, H. S., Gohar, Y. M. 2016.Protective effect of squilla chitosan–silver nanoparticles for Dicentrarchus labrax. International Aquatic Research., 8(2): 179-189.

Baram-Pinto, D., Shukla, S., Perkas, N., Gedanken, A., Sarid, R. 2009. Inhibition of herpes simplex virus type 1 infection by silver nanoparticles capped with mercaptoethane sulfonate. Bioconjugate Chem, 20: 1497–1502.

Bartlett, A. H., Foster, T. J., Hayashida, A., Park, P. W. 2008. α-toxin facilitates the generation of CXC chemokine gradients and stimulates neutrophil homing in *Staphylococcus aureus* pneumonia. Journal of Infectious Diseases, 198(10): 1529–1535.

Basset, P., Feil, E.J., Zanetti, G., Blanc, D.S. 2011. 25 - The Evolution and Dynamics of Methicillin-Resistant *Staphylococcus aureus*. In M. Tibayrenc (Ed.), Genetics and Evolution of Infectious Disease, 669-688.

Bindhu, M.R., and Umadevi, M. 2014. Silver and gold nanoparticles for sensor and antibacterial applications. Spectrochimica Acta Part A: Molecular and Biomolecular Spectroscopy, 128: 37-45.

Bischoff, M., Entenza, J.M., 2001. Giachino P. Influence of a functional sigB operon on the global regulators sar and agr in *Staphylococcus aureus* . Journal of Bacteriology. 183(17): 5171–5179.

Bokarewa, M.I., Jin, T., Tarkowski, 2006. A. *Staphylococcus aureus*: staphylokinase. International Journal of Biochemistry and Cell Biology. 38(4): 504–509.

Caballero, A.R., Tang, A., Bierdeman, M., O'Callaghan, R., Marquart, M. 2021. Correlation of Staphylococcus epidermidis Phenotype and Its Corneal Virulence.Curr. Eye Res. 46: 638–647.

Chavakis, T., Hussain, M., Kanse, S.M., 2002. *Staphylococcus aureus* extracellular adherence protein serves as anti-inflammatory factor by inhibiting the recruitment of host leukocytes. Nature Medicine, 8(7): 687–693.

Cheung, A.L., Bayer, A.S., Zhang, G., Gresham, H., Xiong, Y.Q.2004. Regulation of virulence determinants in vitro and in vivo in *Staphylococcus aureus* . FEMS Immunology and Medical Microbiology. 40(1): 1–9.

Cheung, A.L., Projan, S.J., Gresham, H. 2002. The genomic aspect of virulence, sepsis, and resistance to killing mechanisms in *Staphylococcus aureus* . Current Infectious Disease Reports. 4: 400–410.

Cheung, A.L., Schmidt, K., Bateman, B., Manna, A.C. 2001. SarS, a SarA homolog repressible by agr, is an activator of protein a synthesis in *Staphylococcus aureus*. Infection and Immunity. 69(4): 2448–2455.

Cho, K.H., Park, J.E., Osaka, T., Park, S.G. 2005. The study of antimicrobial activity and preservative effects of nanosilver ingredient. Electrochim Acta, 51: 956–960.

Choi, O., Deng, K.K., Kim, N.J., Ross, L., Surampalli, R.Y. and Hu, Z. 2008. Theinhibitory effects of silver nanoparticles, silver ions, and silver chloride colloids on microbial growth. Water Research, (42): 3066-3074.

Chuang, Y.Y., Huang, Y.C. 2013. Molecular epidemiology of community-associated meticillin-resistant *Staphylococcus aureus* in Asia. The Lancet Infectious Diseases, 13(8): 698-708.

Chung, I.M., Park, I., Seung-Hyun, K., Thiruvengadam, M., Rajakumar, G. 2016. Plant-Mediated Synthesis of Silver Nanoparticles: Their Characteristic Properties and Therapeutic Applications. Nanoscale Res. Lett. 11: 1–14.

Cordeiro, L., Figueiredo, P., Souza, H., Sousa, A., Andrade-Júnior, F., Medeiros, D., Nóbrega, J., Silva, D., Martins, E., BarbosaFilho, J. 2020. Terpinen-4-ol as an Antibacterial and Antibiofilm Agent against *Staphylococcus aureus*.Int. J. Mol. Sci. 21: 4531.

Courrol, D.D.S., Lopes, C.R.B., Pereira, C.B.P., Franzolin, M.R., Silva, F.R.O., Courrol, L.C. 2019. Tryptophan Silver Nanoparticles Synthesized by Photoreduction Method: Characterization and Determination of Bactericidal and Anti-Biofilm Activities on Resistant and Susceptible Bacteria. Int. J. Tryptophan Res. 12: 1178646919831677.

Dang, T.M.D., Le, T.T.T., Fribourg-Blanc, E., Dang, M.C. 2012. Influence of surfactant on the preparation of silver nanoparticles by polyol method. Adv. Nat. Sci. Nanosci. Nanotechnol. 3: 035004.

De Haas, C.J.C., Veldkamp, K.E., Peschel, A. 2004. Chemotaxis inhibitory protein of *Staphylococcus aureus*, a bacterial antiinflammatory agent. Journal of Experimental Medicine. 199(5): 687–695.

den Heijer, C.D.J., van Bijnen, E.M.E., Paget, W.J., Pringle, M., Goossens, H., Bruggeman, C.A., Stobberingh, E.E. 2013. Prevalence and resistance of commensal *Staphylococcus aureus*, including meticillin-resistant S aureus, in nine European countries: a cross-sectional study. The Lancet Infectious Diseases.13(5), 409-415.

Dinges, M.M., Orwin, P.M., Schlievert, P.M. 2000. Exotoxins of *Staphylococcus aureus* . Clinical Microbiology Reviews. 13(1): 16–34.

Doskar, J., Pantůček, R., Růžičková, V., Sedláček, I. 2010. Molecular Diagnostics of *Staphylococcus aureus* Detection of Bacteria, Viruses, Parasites and Fungi, Springer, 139-184.

Durán, N., Nakazato, G., Seabra, A. 2016. Antimicrobial activity of biogenic silver nanoparticles, and silver chloride nanoparticles: an overview and comments. Appl Microbiol Biotechnol. 100(15): 6555–6570.

Elsupikhe, R.F., Shameli, K., Ahmad, M.B., Ibrahim, N.A., Zainudin, N. 2015. Green sonochemical synthesis of silver nanoparticles at varying concentrations of κ-carrageenan. Nanoscale Res. Lett. 10: 1–8.

El-Zahry, M.R., Mahmoud, A., Refaat, I.H., Mohamed, H.A., Bohlmann, H., Lendl, B. 2015. Antibacterial effect of various shapes of silver nanoparticles monitored by SERS. Talanta. 138: 183–189.

Fernandes, L.F., Souza, G., Almeida, A.C., Cardoso, L., Xavier, M., Pinheiro, T., Cruz, G., Dourado, H., Silva, W.S., Xavier, A. 2020. Identification and characterization of methicillin-resistant Staphylococcus spp. isolated from surfaces near patients in an intensive care unit of a hospital in southeastern Brazil. Rev. Soc. Bras. Med., 53: e20200244.

Ferry T, Perpoint T, Vandenesch F, Etienne J. 2005. Virulence determinants in *Staphylococcus aureus* and their involvement in clinical syndromes. Current Infectious Disease Reports. 7(6): 420–428.

Flock JI, Fröman G, Jönsson K. 1987. Cloning and expression of the gene for a fibronectin-binding protein from *Staphylococcus aureus*. EMBO Journal. 6(8): 2351–2357.

Forbes, B., Sahm, D. and Weissfeld, A. 2016. Baily and Scott Diagnostic Microbiology. (14thed.). Mosby Company. Baltimore, USA., 13(1): 19–24.

Foster, T.J., Höök, M. 1996. Surface protein adhesins of *Staphylococcus aureus*. Trends in Microbiology. 6(12):484–488.

Foster, T.J. 2005. Immune evasion by staphylococci.Nature Reviews Microbiology. 3(12):948–958.

Fournier, B., Hooper, D.C. 2000. A new two-component regulatory system involved in adhesion, autolysis, and extracellular proteolytic activity of *Staphylococcus aureus* . Journal of Bacteriology,182(14): 3955–3964.

Fournière, M., Latire, T., Souak, D., Feuilloley, M.G.J., Bedoux, G. 2020. Staphylococcus epidermidis and Cutibacterium acnes: Two Major Sentinels of Skin Microbiota and the Influence of Cosmetics. Microorganisms, 8: 1752.

Franke S, Grass G, Nies DH 2001. The product of the ybdE gene of the Escherichia coli chromosome is involved in detoxification of silver ions. Microbiology 147:965–972.

Gardea-Torresdey, J.L., Gomez, E., Peralta-Videa, J.R., Parsons, J.G., Troiani, H., and Jose-Yacaman, M. 2003. Alfalfa sprouts: a natural source for the synthesis of silver nanoparticles. Langmuir, (19): 1357-1361.

Giraudo AT, Raspanti CG, Calzolari A, Nagel R. Characterization of a Tn551-mutant of *Staphylococcus aureus* defective in the production of several exoproteins. Canadian Journal of Microbiology. 40(8): 677–681.

Gonzalez-Martina, M., Corberaa, J.A., Suarez-Bonnetb, A., Tejedor-Junco, M.T. 2020. Virulence factors in coagulase-positive staphylococci of veterinary interest other than *Staphylococcus aureus*. Vet. Q. 40: 118–131.

Guo, Y., Song, G., Sun, M., Wang, J., Wang, Y. 2020. Prevalence and Therapies of Antibiotic-Resistance in *Staphylococcus aureus*. Front. Cell. Infect. 10: 107.

Gurunathan, S., Kalishwaralal, K., Vaidyanathan, R., Venkataraman, D., Pandian, S.R.K., Muniyandi, J., Hariharan, N., Eom, S.H. 2009. Biosynthesis, purification and characterization of silver nanoparticles using Escherichia coli. Colloids Surf. B Biointerfaces, 74: 328–335.

Guzman, M., Dille, J. and Godet, S. 2011. Synthesis and antibacterial activity of silver nanoparticles against gram-positive and gram-negative bacteria. Nanomedicine: Nanotechnology, Biology and medicine. (8): 37-45.

Habash, M.B., Goodyear, M.C., Park, A.J., Surette, M.D., Vis, E.C., Harris, R.J., Khursigara, C.M. 2017. Potentiation of tobramycin by silver nanoparticles against Pseudomonas aeruginosa biofilms. Antimicrob.Agents Chemother. 61: e00415-17.

Haiyan, Yu., H., Haoyu Sun, H., 2019. Chunsheng Yin, C., Zhifen Lin, Z. Combination of sulfonamides, silver antimicrobial agents and quorum sensing inhibitors as a preferred approach for improving antimicrobial efficacy against Bacillus subtilis. Ecotoxicol. Environ. Saf., 181: 43–48.

Hayashida, A., Bartlett, A.H., Foster, T.J., Park, P.W. 2009. *Staphylococcus aureus* beta-toxin induces lung injury through syndecan-1. American Journal of Pathology. 174(2): 509–518.

Hildebrand, A. 1991. Pohl M, Bhakdi S. *Staphylococcus aureus*α-toxin: dual mechanism of binding to target cells. Journal of Biological Chemistry. 266(26):17195–17200.

Holden, M.T.G., Feil, E.J., Lindsay, J.A., Peacock, S.J., Day, N.P.J., Enright, M.C., Atkin, R. 2004. Complete genomes of two clinical *Staphylococcus aureus* strains: evidence for the rapid evolution of virulence and drug resistance. Proceedings of the National Academy of Sciences of the United States of America, 101(26): 9786-9791.

Holmes A, Ganner M, McGuane S, Pitt TL, Cookson BD, Kearns AM. *Staphylococcus aureus* isolates carrying panton-valentine leucocidin genes in England and Wales: frequency, characterization, and association with clinical disease. Journal of Clinical Microbiology. 2005,43(5):2384–2390.

Holtfreter S, Bröker BM. Staphylococcal superantigens: do they play a role in sepsis? Archivum Immunologiae et Therapiae Experimentalis. 2005,53(1):13–27.

Husmann M, Dersch K, Bobkiewicz W, Beckmann E, Veerachato G, Bhakdi S. Differential role of p38 mitogen activated protein kinase for cellular recovery from

attack by pore-forming *S. aureus* alpha-toxin or streptolysin O. Biochemical and Biophysical Research Communications. 2006, 344:1128–1134.

Jacob JM, John MS, Jacob A, *et al.* Bactericidal coating of paper towels via sustainable biosynthesis of silver nanoparticles using ocimum sanctum leaf extract. Bactericidal Coat Pap Towels Sustainable Biosynth Silver Nanopart Ocimum Sanctum Leaf Extr. 2019,6(4): 045401.

Jara, P., Herrera, B., Yutronic, N. 2015. Formation of Nanoparticles and Decoration of Organic Crystals. In Handbook of Nanoparticles, Aliofkhazraei, M., Ed., Springer International Publishing: Cham, Switzerland, 4: 1–14.

Jeevanandam, J., Krishnan, S., Hii, Y.S., Pan, S., Chan, Y.S., Acquah, C., Danquah, M.K., Rodrigues, J. Synthesis approachdependent antiviral properties of silver nanoparticles and nanocomposites. J. Nanostruct. Chem. 2022, 1–23.

Jevons, M.P. 1961. 'Celbenin'–resistant staphylococci, British Medical Journal, 124: 124–5.

Jung WK, Koo HC, Kim KW, Shin S, Kim SH, Park YH (2008) Antibacterial activity and mechanism of action of the silver ion in *Staphylococcus aureus* and Escherichia coli. Appl Environ Microbiol 74(7):2171–2178.

Kaneko J, Kamio Y. Bacterial two-component and hetero-heptameric pore-forming cytolytic toxins: structures pore-forming mechanism organization of the genes. Bioscience, Biotechnology, and Biochemistry. 2004,68:981–1003.

Khan, R.A.G., Khan, F.A. and Khan, M.A. (2011) Impact of Training and Development on Organizational Performance. Global Journal of Management and Business Research, 11, 62-68.

Khorrami S, Jafari F, Zarrabi A, Zarepour A. Is Astragalus gossypinus honey a natural antibacterial and cytotoxic agent? An investigation on A. gossypinus honey biological activity and its green synthesized silver nanoparticles. Bionanosci. 2018,9(3):603–10.

Khorrami S, Zarrabi A, Khaleghi M, Danaei M, Mozafari M. Selective cytotoxicity of green synthesized silver nanoparticles against the MCF-7 tumor cell line and their enhanced antioxidant and antimicrobial properties. Int J Nanomedicine. 2018,13:8013–8024.

Kim JS, Kuk E, Yu KN, Kim JH, Park SJ and Lee HJ. Antimicrobial effects of silver nanoparticles. Nanomedicine: Nanotechnology, Biology and Medicine, 2007 (3):95-101.

Kim JS, Kuk E, Yu KN, Kim JH, Park SJ, Lee HJ, Kim SH, Park YK, Park YH, Hwang CY, Kim YK, Lee YS, Jeong DH, Cho MH (2007) Antimicrobial effects of silver nanoparticles. Nanomedicine: Nanotechnol Biol Med 3(1):95–101.

Kim KJ, Sung WS, Suh BK, Moon SK, Choi JS, Kim JG, Lee DG (2009) Antifungal activity and mode of action of silver nanoparticles on Candida albicans. Biometals 22:235–242.

Klaus-Joerger, T., Joerger, R., Olsson, E., Granqvist, C.-G. Bacteria as workers in the living factory: Metal-accumulating bacteria and their potential for materials science. Trends Biotechnol. 2001, 19, 15–20.

Koch, J.A., Pust, T.M., Cappellini, A.J., Mandell, J.B., Ma, D., Shah, N.B., Brothers, K.M., Urish, K.L. Staphylococcus epidermidis Biofilms Have a High Tolerance to Antibiotics in Periprosthetic Joint Infection. Life 2020, 10, 253.

Korshed, P., Li, L., Liu, Z., Mironov, A., Wang, T. Size-dependent antibacterial activity for laser-generated silver nanoparticles. J. Interdiscip. Nanomed. 2019, 4, 24–33.

Kreis T, Vale R. Guidebook to the Extracellular Matrix, Anchor, and Adhesion Proteins. Oxford, UK: Oxford University Press, 1999.

Krutyakov, Y.A., Kudrinskiy, A.A., Olenin, A.Y., Lisichkin, G. V Synthesis and properties of silver nanoparticles: Advances and prospects. Russ. Chem. Rev. 2008, 77, 233–257.

Kulkarni, S.K. Nanotechnology—Principles and Practices, 3rd ed., Springer: Berlin, Germany, 2014, ISBN 9783319091709.

Kumar VP, Pammi S, Kollu P, Satyanarayana K, and Shameem U. Green synthesis and characterisation of silver nanoparticles using. Boerhaavia diffusa plant extract and their antibacterial activity. Industrial Crops and Products, 2014, (52): 562-566.

Kuppusamy, P., Yusoff, M.M., Maniam, G.P., Govindan, N. Biosynthesis of metallic nanoparticles using plant derivatives and their new avenues in pharmacological applications--An updated report. Saudi Pharm. J. 2016, 24, 473–484.

Lara HH, Ayala-Nun˜ez NV, Ixtepan-Turrent L, RodriguezPadilla C (2010) Mode of antiviral action of silver nanoparticles against HIV-1. J Nanobiotechnol 8:1–10.

Lara, H. H., Ayala-Núnez, N. V., Turrent, L. D. C. I ,.andPadilla, C. R. (2010). Bactericidal effect of silver nanoparticles against multidrug-resistant bacteria.World Journal of Microbiology and Biotechnology.(26), 615-621.

Law N, Ansari S, Livens FR, Renshaw JC, Lloyd JR (2008) Formation of nanoscale elemental silver particles via enzymatic reduction by Geobacter sulfurreducens. Appl Environ Microbiol 74(22):7090–7093.

Lee BU, Yun SH, Ji JH, Bae GN (2008) Inactivation of S. epidermidis, B. subtilis, and E. coli bacteria bioaerosols deposited on a filter utilizing airborne silver nanoparticles. J Microbiol Biotechnol 18(1):176–182.

Lee LYL, Liang X, Höök M, Brown EL. Identification and characterization of the C3 binding domain of the *Staphylococcus aureus* extracellular fibrinogen-binding protein (Efb) Journal of Biological Chemistry. 2004,279(49):50710–50716.

Leng, D., Li, Y., Zhu, J., Liang, R., Zhang, C., Zhou, Y., Li, M., Wang, Y., Rong, D., Wu, D., *et al.*The Antibiofilm Activity and Mechanism of Nanosilver- and Nanozinc-Incorporated Mesoporous Calcium-Silicate Nanoparticles. Int. J. Nanomed. 2020, 15, 3921–3936

Li L, Zhou X, *et al.* Silver nanoparticles induce protective autophagy via Ca 2+ /CaMKKβ/AMPK/mTOR pathway in SH-SY5Y cells and rat brains. Nanotoxicology. 2019,13(3):369–391.

Li WR, Xie XB, Shi QS, Zeng HY, Ou-Yang YS, Chen YB (2010) Antibacterial activity and mechanism of silver nanoparticles on Escherichia coli. Appl Microbiol Biotechnol 85:1115–1122.

Liao C, Li Y, Tjong SC. Bactericidal and cytotoxic properties of silver nanoparticles. Int J Mol Sci. 2019,20(2):449.

Lina G, Bohach GA, Nair SP, Hiramatsu K, Jouvin-Marche E, Mariuzza R. Standard nomenclature for the superantigens expressed by Staphylococcus. Journal of Infectious Diseases. 2004,189(12):2334–2336.

Lok CN, Ho CM, Chen R, He QY, Yu WY, Sun H, Tam PK, Chiu JF, Chen CM (2006) Proteomic analysis of the mode of antibacterial action of silver nanoparticles. J Proteome Res 5:916–924.

Lowy FD. *Staphylococcus aureus* infections. The New England Journal of Medicine. 1998,339:520–532.

Lu L, Sun RW, Chen R, Hui CK, Ho CM, Luk JM, Lau GK, Che CM (2008) Silver nanoparticles inhibit hepatitis B virus replication. Antivir Ther 13:253–262.

Luzzago, C., Locatelli, C., Franco, A., Scaccabarozzi, L., Gualdi, V., Viganò, R., Sironi, G., Besozzi, M., Castiglioni, B., Lanfranchi, P. and Cremonesi, P. 2014. Clonal diversity, virulence-associated genes and antimicrobial resistance profile of *Staphylococcus aureus* isolates from nasal cavities and soft tissue infections in wild ruminants in Italian Alps. Veterinary Microbiology, 170(1):157-61.

Maresso AW, Schneewind O. Sortase as a target of anti-infective therapy. Pharmacological Reviews. 2008,60(1):128–141.

Markey, P. M., Markey, C. N., and French, J. E. (2015). Violent video games and real-world violence: Rhetoric versus data. Psychology of Popular Media Culture, 4(4), 277–295. https://doi.org/10.1037/ppm0000030

Meikle T, Dyett BP, Strachan JB, White J, Drummond CJ, Conn CE. Preparation, characterization, and antimicrobial activity of cubosome encapsulated metal nanocrystals. ACS Appl Mater Interfaces. 2020,12(6):6944–6954.

Melish ME, Glasgow LA.The staphylococcal scalded-skin syndrome. New England Journal of Medicine. 1970,282(20):1114–1119.

Menestrina G, Dalla Serra M, Prévost G. Mode of action of β-barrel pore-forming toxins of the staphylococcal α-hemolysin family. Toxicon. 2001,39(11):1661–1672.

Mittal AK, Bhaumik J, Kumar S, and Banerjee, UC. Biosynthesis of silver nanoparticles: elucidation of prospective mechanism and therapeutic potential. Journal of Colloid Interface Science 2014(415): 39-47.

Morlock BA, Spero L, Johnson AD. Mitogenic activity of staphylococcal exfoliative toxin. Infection and Immunity. 1980,30(2):381–384.

Naidu Krishna, S., Govender, P., Adam, J.K. 2015. Nano silver particles in biomedical and clinical applications. J. Pure Appl. Microbiol. 19(15): 20–24.

Nakamura, T., Magara, H., Herbani, Y., Sato, S. Fabrication of silver nanoparticles by highly intense laser irradiation of aqueous solution. Appl. Phys. A Mater. Sci. Process. 2011, 104, 1021–1024.

Nam, K.T., Lee, Y.J., Krauland, E.M., Kottmann, S.T., Belcher, A.M. Peptide-mediated reduction of silver ions on engineered biological scaffolds. ACS Nano 2008, 2, 1480–1486

Narayanan, K.B., Park, H.H. Antifungal activity of silver nanoparticles synthesized using turnip leaf extract (Brassica rapa L.) against wood rotting pathogens. Eur. J. Plant Pathol. 2014, 140, 185–192.

Noronha VT, Paula AJ, Durán G, *et al.* Silver nanoparticles in dentistry. Dent Mater. 2017,33(10):1110–1126.

Noto, M.J., Fox, P.M. and Archer, G.L. 2008. Spontaneous deletion of the methicillin resistance determinant, mecA, partially compensates for the fitness cost associated with high-level vancomycin resistance in *Staphylococcus aureus*. Antimicrobial Agents and Chemotherapy, 52: 1221-1229.

Olaleye, M.T., Akinmoladun, A.C., Ogunboye, A.A., Akindahunsi, A.A. Antioxidant activity and hepatoprotective property of leaf extracts of Boerhaavia diffusa Linn against acetaminophen-induced liver damage in rats.Food Chem. Toxicol. 2010, 48, 2200–2205.

Pal, S., Tak, Y.K., Song, J.M. Does the antibacterial activity of silver nanoparticles depend on the shape of the nanoparticle? A study of the Gram-negative bacterium Escherichia coli. Appl. Environ. Microbiol. 2007, 73, 1712–1720.

Parashar V, Parashar R, Sharma B, and Pandey AC. Parthenium leaf extract mediated synthesis of silver nanoparticles: a novel approach towards weed utilisation. Digest Journal of Nanomaterials and Biostructures. 2009(4): 45-50.

Peng HL, Novick RP, Kreiswirth B, Kornblum J, Schlievert P. Cloning, characterization and sequencing of an accessory gene regulator (agr) in *Staphylococcus aureus* . Journal of Bacteriology. 1988,170(9):4365–4372.

Plata, K., Rosato, A.E. and Wegrzyn, G. 2009. *Staphylococcus aureus* as an infectious agent: overview of biochemistry and molecular genetics of its pathogenicity. Acta Biochimica Polonica, 56(4): 597.

Platania, V., Kaldeli-Kerou, A., Karamanidou, T., Kouki, M., Tsouknidas, A., Chatzinikolaidou, M. Antibacterial Effect of Colloidal Suspensions Varying in Silver Nanoparticles and Ions Concentrations.Nanomaterials 2021, 12, 31.

Prat C, Bestebroer J, De Haas CJC, Van Strijp JAG, Van Kessel KPM. A new staphylococcal anti-inflammatory protein that antagonizes the formyl peptide receptor-like 1. Journal of Immunology. 2006,177(11):8017–8026.

Pugazhendhi A, Prabakar D, Jacob JM, Karuppusamy I, Saratale RG. Synthesis and characterization of silver nanoparticles using Gelidium amansii and its antimicrobial property against various pathogenic bacteria. Microb Pathog. 2018,114:41–45.

Purrello, S.M., Daum, R.S., Edwards, G.F.S., Lina, G., Lindsay, J., Peters, G., Stefani, S. 2012. Meticillin-resistant *Staphylococcus aureus* (MRSA) update: New insights into bacterial adaptation and therapeutic targets. Journal of Global Antimicrobial Resistance, 2(2): 61-69.

Quinn, P.J., Carter, M.E., Markey, B. and Carter, G.R. 2004.Clinical Veterinary Microbiology. 6th Ed. Mosby an imp. Wolf, London, 1: 16–20.

Rai M, Yadav A, Gade A (2009) Silver nanoparticles as a new generation of antimicrobials. Biotechnol Adv 27:76–83.

Ramkumar VS, Pugazhendhi A, Gopalakrishnan K, *et al.* Biofabrication and characterization of silver nanoparticles using aqueous extract of seaweed, 16–34.

Renugadevi K, and Aswini RV. Microwave irradiation assisted synthesis of silver nanoparticles using Azadirachta indica leaf extract as a reducing agent and In vitro evaluation of its antibacterial and anticancer activity. International Journal of Nanomaterials and Biostructures 2012, 2: 5-10.

Rogers JV, Parkinson CV, Choi YW, Speshock JL, Hussain SM (2008) A preliminary assessment of silver nanoparticle inhibition of monkeypox virus plaque formation. Nanoscale Res Lett 3:129–133.

Rooijakkers SHM, Ruyken M, Roos A, *et al.* Immune evasion by a staphylococcal complement inhibitor that acts on C3 convertases.Nature Immunology. 2005,6(9):920–927.

Sadeghi B, Garmaroudi FS, Hashemi M, Nezhad H, Nasrollahi A and Ardalan S. Comparison of the antibacterial activity on the nanosilver shapes: nanoparticles, nanorods and nanoplates. Advanced Powder Technology. 2012 (23): 22-26.

Saleha, A., Zunita, Z. 2010. Methicillin resistant *Staphylococcus aureus* (MRSA): An emerging veterinary and zoonotic pathogen of public health concern and some studies in Malaysia. Journal Animal Veterinary Advances, 9(7): 1094-1098.

Sameer J Nadafa, Sandip Bandgar, Indrayani D Raut, In Sabu T and Balakrishnan P. Nanostructures for antimcrobial therapy., Nanoscale Processing, Elsevier Book. Amsterdam, Netherlands. 2021, 362-375.

Sanghi, R., Verma, P. Biomimetic synthesis and characterisation of protein capped silver nanoparticles. Bioresour. Technol. 2009, 100, 501–504.

Saravanan M, Arokiyaraj S, Lakshmi T, Pugazhendhi A. Synthesis of silver nanoparticles from Phenerochaete chrysosporium (MTCC-787) and their antibacterial activity against human pathogenic bacteria. Microb Pathog. 2018,117:68–72. doi:10.1016/j.micpath.2018.02.008

Senapati, S., Ahmad, A., Khan, M.I., Sastry, M., Kumar, R. Extracellular biosynthesis of bimetallic Au–Ag alloy nanoparticles. Small 2005, 1, 517–520.

Shanmuganathan R, MubarakAli D, Prabakar D, *et al.* An enhancement of antimicrobial efficacy of biogenic and ceftriaxone-conjugated silver nanoparticles: green approach. Environ Sci Pollut Res Int. 2018,25(11):10362–10370.

Shaw, L., Golonka, E., Potempa, J. and Foster, S.J. 2004. The role and regulation of the extracellular proteases of *Staphylococcus aureus*. Microbiology, 150(1): 217-228.

Silva, L.P., Silveira, A.P., Bonatto, C.C., Reis, I.G., Milreu, P.V. Silver Nanoparticles as Antimicrobial Agents: Past, Present, and Future. In Nanostructures for Antimicrobial Therapy: Nanostructures in Therapeutic Medicine Series, Elsevier: Amsterdam, The Netherlands, 2017, pp. 577–596.

Silver S (2003) Bacterial silver resistance: molecular biology and uses and misuses of silver compounds. FEMS Microbiol Rev 27:341–353.

Silver S, Phung LT, Silver G (2006) Silver as biocides in burn and wound dressings and bacterial resistance to silver compounds. J Ind Microbiol Biotechnol 33:627–634.

Sivaramasamy E, Zhiwei W, Li F, Xiang J. Enhancement of Vibriosis Resistance in Litopenaeus vannamei by Supplementation of Biomastered Silver Nanoparticles by Bacillus subtilis. Journal of Nanomedicine Nanotechnology. 2016, 7(352):2.

Słowik, R., Kołpa, M., Wałaszek, M., Róza ´nska, A., Jagiencarz-Starzec, B., Zie ´nczuk, W., Kawik, Ł., Wolak, Z., W ˙ ójkowska-Mach, J. Epidemiology of Surgical Site Infections Considering the NHSN Standardized Infection Ratio in Hip and Knee Arthroplasties. Int. J. Environ. Res. 2020, 17, 3167.

Sondi I, Salopek-Sondi B (2004) Silver nanoparticles as antimicrobial agent: a case study on E. coli as a model for Gram-negative bacteria. J Colloid Interface Sci 275: 177–182.

Sondi, I., Salopek-Sondi, B. Silver nanoparticles as antimicrobial agent: A case study on E. coli as a model for Gram-negative bacteria. J. Colloid Interface Sci. 2004, 275, 177–182.

Speziale P, Pietrocola G, Rindi S, *et al.* Structural and functional role of *Staphylococcus aureus* surface components recognizing adhesive matrix molecules of the host. Future Microbiology. 2009,4(10):1337–1352.

Sun RW, Chen R, Chung NP, Ho CM, Lin CL, Che CM (2005) Silver nanoparticles fabricated in Hepes buffer exhibit cytoprotective activities toward HIV-1 infected cells. Chem Comm 40:5059–5061.

Suriyakalaa, U., Antony, J.J., Suganya, S., Siva, D., Sukirtha, R., Kamalakkannan, S., Pichiah, P.B.T., Achiraman, S. Hepatocurative activity of biosynthesized silver nanoparticles fabricated using Andrographis paniculata. Colloids Surf. B Biointerfaces 2013, 102, 189–194.

Tanvir, F., Yaqub, A., Tanvir, S., Anderson, W.A. Poly-L-arginine Coated Silver Nanoprisms and Their Anti-Bacterial Properties.Nanomaterials 2017, 7, 296.

Tegmark K, Karlsson A, Arvidson S. Identification and characterization of SarH1, a new global regulator of virulence gene expression in *Staphylococcus aureus* . Molecular Microbiology. 2000,37(2):398–409.

Thomas V, Yallapu MM, Sreedhar B, Bajpai SK (2007) A versatile strategy to fabricate hydrogel-silver nanocomposites and investigation of their antimicrobial activity. J Colloid Interface Sci 315:389–395.

Torres VJ, Attia AS, Mason WJ, *et al. Staphylococcus aureus* fur regulates the expression of virulence factors that contribute to the pathogenesis of pneumonia. Infection and Immunity. 2010,78(4):1618–1628.

Tran, Q.H., Nguyen, V.Q., Le, A. Silver nanoparticles: Synthesis, properties, toxicology, applications and perspectives. Adv. Nat. Sci. Nanosci. Nanotechnol.2013, 4, 033001.

Turnidge, J., Chang, F.Y., Fowler, V.G. and Rao, N. 2008.*Staphylococcus aureus*.Updated December.Guided Medline Search. http://www. antimicrobe.org/sample_staphylococcus.asp Last accessed August 29, 2018.

Tuševljak N, Dutil L, Rajić A, UHLAnd FC, McClure C, St-Hilaire S *et al.* Antimicrobial use and resistance in aquaculture: findings of a globally administered survey of aquaculture-allied professionals. Zoonoses and public health, 2013, 60(6):426-436.

Vaseeharan B, Ramasamy P, Chen JC. Antibacterial activity of silver nanoparticles (AgNPs) synthesised by tea leaf extracts against pathogenic Vibrio harveyi and its protective efficacy on juvenile Feneropenaeus indicus. Letters in applied microbiology. 2010, 50(4):352-356.

Wang, P.J., Xie, C.B., Sun, F.H., Guo, L.J., Dai, M., Cheng, X., Ma, Y.X. Molecular Characteristics of Methicillin-Resistant Staphylococcus epidermidis on the Abdominal Skin of Females before Laparotomy.Int. J. Mol. Sci. 2016, 17, 992.

Wardenburg JB, Schneewind O. Vaccine protection against *Staphylococcus aureus* pneumonia. Journal of Experimental Medicine. 2008,205(2):287–294.

Wilke GA, Wardenburg JB. Role of a disintegrin and metalloprotease 10 in *Staphylococcus aureus*α-hemolysin—mediated cellular injury. Proceedings of the National Academy of Sciences of the United States of America. 2010,107(30):13473–13478.

Yamanaka M, Hara K, Kudo J (2005) Bactericidal actions of a silver ion solution on Escherichia coli, studied by energyfiltering transmission electron microscopy and proteomic analysis. Appl Environ Microbiol 71(11):7589–7593.

Yaqoob, A.A., Umar, K., Ibrahim, M.N.M. Silver nanoparticles: Various methods of synthesis, size affecting factors and their potential applications—A review. Appl. Nanosci. 2020, 10, 1369–1378.

Yin IX, Yu OY, Zhao IS, *et al.* Developing biocompatible silver nanoparticles using epigallocatechin gallate for dental use. Arch Oral Biol. 2019,102:106–112. doi:10.1016/j.archoralbio.2019.03.022

Yoon KY, Byeon JH, Park JH, Hwang J (2007) Susceptibility constants of Escherichia coli and Bacillus subtilis to silver and copper nanoparticles. Sci Total Environ 373:572–575.

Zhang, X.F., Liu, Z.G., Shen, W., Gurunathan, S. Silver nanoparticles: Synthesis, characterization, properties, applications, and therapeutic approaches. Int. J. Mol. Sci. 2016, 17, 1534.

Zhao GJ, Stevens SE (1998) Multiple parameters for the comprehensive evaluation of the susceptibility of Escherichia coli to the silver ion. Biometals 11:27–32

APPENDICES

APPENDIX 1.Approval of the Iraqi Ministry of Health to implement the project

APPENDIX 2.Editing certificate

Appendix 1. Approval of the Iraqi Ministry of Health to implement the project

Appendix 2.Editing certificate

CURRICULUM VITAE

Personal Information

Name and Surname : AI- Hasan Ali Yousif AL- ABAYECHI

Education

MSc	Çankırı Karatekin University Graduate School of Natural and Applied Sciences Department of Biology	2021-2023
Undergraduate	Thi-Qar University Faculty of Natural and Applied Sciences Pathological analyzes	2016-2020